Published in final edited form as:

Mol Microbiol. 2016 April ; 100(1): 90–107. doi:10.1111/mmi.13303.

An orphaned Mce-associated membrane protein of *Mycobacterium tuberculosis* is a virulence factor that stabilizes Mce transporters

Ellen Foot Perkowski[1], **Brittany K. Miller**[1], **Jessica R. McCann**[1,*], **Jonathan Tabb Sullivan**[1,^], **Seidu Malik**[1], **Irving Coy Allen**[2], **Virginia Godfrey**[3], **Jennifer D. Hayden**[1], and **Miriam Braunstein**[1,#]

[1]Department of Microbiology and Immunology, University of North Carolina

[2]Department of Biomedical Sciences and Pathobiology, University of North Carolina

[3]Virginia-Maryland College of Veterinary Medicine, Department of Pathology and Laboratory Medicine, University of North Carolina

Summary

Mycobacterium tuberculosis proteins that are exported out of the bacterial cytoplasm are ideally positioned to be virulence factors; however, the functions of individual exported proteins remain largely unknown. Previous studies identified Rv0199 as an exported membrane protein of unknown function. Here, we characterized the role of Rv0199 in *M. tuberculosis* virulence using an aerosol model of murine infection. Rv0199 appears to be a member of a Mce-associated membrane (Mam) protein family leading us to rename it OmamA, for orphaned Mce-associated membrane protein A. Consistent with a role in Mce transport, we showed OmamA is required for cholesterol import, which is a Mce4-dependent process. We further demonstrated a function for OmamA in stabilizing protein components of the Mce1 transporter complex. These results indicate a function of OmamA in multiple Mce transporters and one that may be analogous to the role of VirB8 in stabilizing Type IV secretion systems, as structural similarities between Mam proteins and VirB8 proteins are predicted by the Phyre 2 program. In this study, we provide functional information about OmamA and shed light on the function of Mam family proteins in Mce transporters.

Keywords

Mycobacterium tuberculosis; Mce; virulence; cholesterol; transporter; Mam

Introduction

Mycobacterium tuberculosis is a human pathogen with a significant impact on world health. Current estimates suggest that 2 billion people worldwide have been infected with *M.*

[#]Address correspondence to Miriam Braunstein: miriam_braunstein@med.unc.edu, (phone) 919-966-5051, (fax) 919-962-8103.
[*]Present address: Department of Pediatrics, Duke University
[^]Integral Molecular, Philadelphia, Pennsylvania

tuberculosis and 1.5 million people die per year from tuberculosis (World Health Organization, 2014). Tuberculosis is spread by inhaled droplets and, upon entering the lungs, *M. tuberculosis* is phagocytosed by macrophages where it then replicates intracellularly. When inside macrophages, *M. tuberculosis* inhibits phagosome maturation and apoptosis, resists reactive radicals, and acquires nutrients through specialized systems (Deretic, 2008; Sturgill-Koszycki *et al.*, 1994; Briken, 2013; Hinchey *et al.*, 2007; Darwin *et al.*, 2003; Niederweis, 2008). In addition, M. tuberculosis produces penetrations in the phagosome membrane providing the pathogen with cytosolic access (van der Wel *et al.*, 2007; Simeone *et al.*, 2015; Manzanillo *et al.*, 2012). While these activities help explain *M. tuberculosis* survival in macrophages, the molecular basis of these events is not clear. Many intracellular pathogens, including *M. tuberculosis*, survive in macrophages with the help of proteins that are exported from the bacterial cytoplasm to the bacterial cytoplasmic membrane, cell wall, or into the host environment.(Ligon *et al.*, 2012; Hicks & Galan, 2013; Isaac & Isberg, 2014). Because of their extracytoplasmic location, exported proteins of pathogens are ideally positioned for host interactions and for specific roles in controlling the immune response and surviving in macrophages (Forrellad *et al.*, 2013; McCann, 2009). While exported proteins are known to play a critical role in *M. tuberculosis* virulence, up to 69% of *M. tuberculosis* exported proteins have no assigned function (Perkowski, E. and Braunstein, M. manuscript in preparation). To better understand how *M. tuberculosis* interacts with the host and causes disease, it is critical to identify the function of exported proteins.

In a previous study using a transposon carrying a β-lactamase reporter of export, the *M. tuberculosis* Rv0199 protein was identified as an exported protein (McCann *et al.*, 2011). Rv0199 is a small 24kDa (219 amino acid) protein with a single TMHMM predicted transmembrane (TM) domain (amino acids 42-64) (Krogh *et al.*, 2001) near its N-terminus (Figure 1A). When fused to a membrane protein, the β-lactamase reporter identifies exported domains that are positioned on the extracytoplasmic side of the membrane by producing β-lactam resistance. The site of the β-lactam resistant transposon insertion in *omamA* produces a hybrid protein with β-lactamase fused at amino acid 74 of OmamA, which indicates the larger C-terminal portion of the protein, following the TM domain, is on the periplasmic/cell wall side of the membrane (Figure 1A) (McCann *et al.*, 2011).

Studies of pooled mutant libraries in macrophages or mice, predict Rv0199 to play a role in virulence (Sassetti & Rubin, 2003; Zhang *et al.*, 2013; Stewart *et al.*, 2005), and experiments directly testing a *rv0199* transposon mutant and complemented strain in cultured macrophages confirm a role for Rv0199 in intracellular growth (McCann *et al.*, 2011). The *rv0199* gene is a core mycobacterial gene (Marmiesse *et al.*, 2004), which means that it is highly conserved throughout pathogenic and non-pathogenic mycobacterial species but not conserved outside of actinomycetes. Yet, the function of Rv0199 is not clear, and Rv0199 is annotated as a membrane protein of unknown function (Lew *et al.*, 2011). There is, however, limited sequence homology between Rv0199 and a family of proteins encoded by genes linked to *mce* operons, which express components of Mce transporters. When first noted, these linked genes were referred to as Mce-associated (*mas*) genes (Casali & Riley, 2007). However, to avoid confusion with the *mas* gene encoding mycocerosic acid synthase of *M. tuberculosis*, we refer to them as Mce-associated membrane (*mam*) genes. Like Rv0199, the

encoded Mam proteins have predicted transmembrane domains near their N-terminus (Perkowski, E. and Braunstein, M. manuscript in preparation). In *M. tuberculosis,* there are eight *mam* genes linked to *mce* operons and an additional five genes encoding proteins with low levels of homology to Mam proteins that are scattered elsewhere in the genome (Figure 1B) (Casali & Riley, 2007). In this report, we will refer to these orphaned *mam* genes as *omam* genes to indicate their unlinked nature. Rv0199 is encoded by one of these orphaned *mam* genes and is referred to as OmamA in this study.

Mce transporters are multi-protein complexes considered to be functionally analogous to ABC transporters (Casali & Riley, 2007). The four Mce transporter systems in *M. tuberculosis* all play roles in virulence (Gioffre *et al.*, 2005; Shimono *et al.*, 2003; Marjanovic *et al.*, 2010; Lima *et al.*, 2007; McCann *et al.*, 2011; Senaratne *et al.*, 2008; Pandey & Sassetti, 2008) and are thought to function in lipid uptake. The best characterized Mce transporter is Mce4. Mce4 is required for cholesterol uptake (Pandey & Sassetti, 2008; Mohn *et al.*, 2008), cholesterol being an important nutrient during *M. tuberculosis* infection (Pandey & Sassetti, 2008). Emerging evidence suggests that Mce1 is responsible for import of mycolic acids, long chain fatty acids characteristic of mycobacteria (Forrellad *et al.*, 2014; Cantrell *et al.*, 2013). Each *mce* operon encodes two YrbE proteins with similarity to ABC transporter permeases and six Mce proteins that are considered functionally similar to substrate binding proteins of ABC transporters (Casali & Riley, 2007). Additionally, Mce transporters are thought to share a common ATPase, MceG. Interestingly, the *mceG* gene is not located near any *mce* operon (Casali & Riley, 2007; Joshi *et al.*, 2006). Nearly all *mce* operons also contain genes encoding Mam proteins (Figure 1B). Unlike the YrbE and Mce components, Mam proteins share no analogous features with ABC transporter components. Mam proteins are speculated to have a role in Mce transporter systems, but this idea is solely based on the genomic location of *mam* genes. To date, there have been no functional studies of any Mam protein. Consequently, the function of potential orphaned Mam proteins such as Rv0199, whose genes are distal to *mce* operons, is even less clear.

Here, we further characterized the role of Rv0199 in *M. tuberculosis* virulence using a low dose aerosol model of murine infection. We additionally showed that Rv0199 has a role in Mce lipid transport, leading us to rename Rv0199 as OmamA (orphaned Mce-associated membrane protein A), and we demonstrated a role for OmamA in stabilizing Mce1 transporter complexes. The stabilization function of OmamA may be analogous to the role of VirB8 in stabilizing Type IV secretion systems, as structural similarities between Mam proteins and VirB8 proteins are predicted by the structural prediction program Phyre 2 (Kelley & Sternberg, 2009). Our results provide important functional information about an exported protein with a role in virulence and provide the first evidence for any Mam protein functioning with Mce transporters. Finally, our results suggest that OmamA, and possibly other Mam proteins as well, have a structural role important for the stability of Mce transporters.

Results

OmamA is important for murine infection

Previous studies revealed a transposon insertion in the *M. tuberculosis rv0199* gene, hereafter referred to as *omamA*, results in a growth defect in resting murine bone-marrow derived macrophages (McCann *et al.*, 2011) and TraSH analysis of a pooled *M. tuberculosis* mutant library in mice predicts a role for OmamA during host infection (Sassetti & Rubin, 2003; Zhang*et al.*, 2013). To further explore the role of the OmamA protein in *M. tuberculosis* infection, we evaluated the course of murine infection with the *omamA* transposon mutant (*omamA::tn*) and compared it to infection with an *omamA*^{WT} strain, hereon referred to as wild type (WT) (McCann*et al.*, 2011). Groups of C57BL/6 mice were infected by low dose aerosol with WT, *omamA::tn*, or a complemented *omamA::tn* +*omamA* strain. Mice infected with the *omamA* mutant had lower bacterial burden in the lungs at 6, 13, and 20 days post-infection compared to WT (Figure 2A). However, by 127 days post-infection there was no longer any difference in bacterial burden in the lungs of mice infected with the *omamA* mutant strain as compared to WT infected mice (Figure 2A). Because aerosol delivered *M. tuberculosis* is not detected in the spleen or liver at the early time points, we quantitated the bacterial burden in these organs at 20 and 127 days post-infection only. The *omamA* infected mice had reduced bacterial burden compared to WT in spleen and liver at 20 days post-infection and, like the burden in the lungs, the number of *omamA* mutant bacteria reached equivalent levels to WT by 127 days post-infection (Figure 2B). Importantly, all defects in bacterial burden were fully restored in mice infected with the complemented strain. These data indicate that OmamA is important for early exponential phase growth in the mouse model of infection.

We also assessed long-term survival of mice infected with the strains described above. The *omamA* mutant infected animals survived significantly longer (>250 days) compared to WT (193 days average) and the complemented strain (173 days average) (Figure 2C). The complemented strain not only alleviated the attenuated phenotype of the *omamA* mutant, but also appeared to potentially accelerate time to death in comparison to WT *M. tuberculosis* (p=0.05). The behavior of the complemented strain may be due to non-physiological levels of OmamA, as the gene is expressed off the constitutive *hsp60* promoter on a multi-copy plasmid.

H&E stained lung sections demonstrated that mice infected with the *omamA* mutant displayed reduced inflammatory infiltration and increased open alveolar spaces in comparison to WT infected mice. The *omamA* mutant showed this reduced histopathology in both early (Day 20) and late (Day 127) timepoints, and the phenotypes were fully restored in the complemented strain (Figure 3A). Blinded scoring of these sections demonstrated that the *omamA* mutant infected mice had lower histopathology scores (histological activity index, HAI) early during infection compared to WT infected mice (Figure 3B). Even after the bacterial burden in *omamA* infected mice caught up to WT levels (Day 127) the HAI scores trended lower in *omamA* mutant infected mice compared to WT infected mice (p=0.07). The lower histopathology of the *omamA* mutant infected mice may help account for their longer survival time in comparison to WT infected mice.

OmamA is an exported protein with predicted structural similarity to VirB8 and Mce-associated membrane proteins

A β-lactamase reporter was previously used to identify OmamA as an exported protein of *M. tuberculosis* (McCann *et al.*, 2011). To confirm the exported nature of OmamA, subcellular fractions of a *Mycobacterium smegmatis* strain engineered to express a C-terminal HA tagged OmamA were prepared for Western blot analysis. OmamA-HA primarily localized to the membrane and cell wall fractions of *M. smegmatis*, with a smaller fraction of OmamA-HA being detected in the soluble fraction, which includes cytoplasmic material (Figure 1C). This result supports the identification of OmamA as an exported protein.

Consistent with a prior bioinformatics analysis (Casali & Riley, 2007), ClustalW2 (Goujon *et al.*, 2010; Thompson *et al.*, 2002) revealed the C-terminal region of OmamA to have a low level of sequence identity (~10-25%) with Mce-associated membrane (Mam) proteins of actinomycetes. Mam proteins are uncharacterized proteins found downstream of *mce* operons (Casali & Riley, 2007). However, the *omamA* gene is not linked to a *mce* operon, leading us to call it an orphaned *mam* gene (*omam*). ClustalW2 reveals 10-25% identity between any two Mam proteins, which is similar to the low homology shared between OmamA and Mam proteins (Supplemental Figure 1). To gain more insight into potential functional domains of the OmamA protein, we used an online 3D structural prediction program Phyre 2 (protein homology/analogy recognition engine version 2.0) (Kelley & Sternberg, 2009). Phyre 2 predicted that the C-terminal domain of OmamA (aa 69-212) folds similarly to NTF2 family proteins (Supplemental Figure 2) (Chaillan-Huntington *et al.*, 2001). Phyre 2 also predicted structural similarity between the C-terminal domain of OmamA and NTF2-like domains in some bacterial proteins. Notable matches were to the structures of VirB8 proteins from *Brucella suis* and *Agrobacterium tumefaciens* and DotI of *Legionella pneumophila* (Figure 1D, Supplemental Figure 2) (Smith *et al.*, 2012; Bailey *et al.*, 2006; Terradot *et al.*, 2005; Kuroda *et al.*, 2015). Like OmamA, VirB8 is a small protein, 26 kDa, with an N-terminal transmembrane domain, and the majority of the protein localized to the periplasm. Additionally, like OmamA, in *B. abortus* VirB8 plays an important role during infection of both mice and macrophages (den Hartigh *et al.*, 2008). VirB8 is a component of the type IV secretion system, a large multi-protein transporter, and it is important to both the stability and function of the transporter complex (Kumar *et al.*, 2000; Sivanesan & Baron, 2011; den Hartigh *et al.*, 2008). DotI is the presumed VirB8 counterpart of the *L. pneumophila* type IV secretion system, Dot/Icm (Kuroda *et al.*, 2015). To determine whether these structural predictions for OmamA are shared with Mam family proteins, we used Phyre 2 to predict the structure of all *M. tuberculosis* Mam proteins. Strikingly, like OmamA, all *M. tuberculosis* Mam family proteins had high confidence structural predictions to NTF2 domain containing proteins, including VirB8 and DotI (Supplemental Figure 2). Given the similarity between the structural predictions of OmamA, Mam and VirB8 proteins, we hypothesized a function of OmamA in Mce transporters, possibly a function analogous to that of VirB8 stabilizing multi-protein transporter complexes.

Deletion of omamA *in* Mycobacterium smegmatis *leads to a* mce *mutant morphology phenotype*

With the goal of assigning a function to OmamA, we first explored the potential for OmamA to contribute to Mce transport in the mycobacterial model organism *M. smegmatis*. *M. smegmatis* has six *mce* operons with nine *mce*-associated *mam* genes and ten orphaned *omam* genes (Casali & Riley, 2007) (Supplemental Figure 3). In *M. smegmatis*, *msmeg0235* is the ortholog of *omamA*, and will be referred to as $omamA_{ms}$. Like $OmamA_{mtb}$, the $OmamA_{ms}$ protein has a predicted transmembrane domain near the N-terminus, and $OmamA_{ms}$ has 55% identity and 76% similarity to $OmamA_{mtb}$ in the C-terminal domain according to BLAST (Altschul *et al.*, 1990). We constructed a deletion mutant of $omamA_{ms}$ and compared phenotypes of the $omamA_{ms}$ mutant to those of *M. smegmatis* mutants lacking *mce4* or all six *M. smegmatis mce* operons (*mce6X*) (Klepp *et al.*, 2012).

Previous studies revealed a rugose morphology for the *mce6X M. smegmatis* mutant growing on Mueller Hinton agar plates containing Congo red (Klepp *et al.*, 2012). Consequently, we tested whether the $omamA_{ms}$ mutant displays a similar morphology. Plates were incubated at 37°C for two days and morphology was assessed by low-magnification microscopy. WT *M. smegmatis* displayed flat, shiny colonies, but *mce4*, *mce6X*, and the $omamA_{ms}$ mutants displayed rugose morphology (Figure 4). The rugose phenotype of the $omamA_{ms}$ mutant could be complemented by either expression of $omamA_{mtb}$ or $omamA_{ms}$ from a plasmid (Figure 4). While the basis of the *mce* mutant rugose phenotype is not currently understood, the appearance of a similar phenotype for the $omamA_{ms}$ *M. smegmatis* mutant is consistent with a role for OmamA in Mce transporters.

Double mutants $omamA_{ms}mce4$ and $omamA_{ms}mce6X$ mutants were also constructed and tested for possible epistatic interactions. Double mutants were spotted and compared to single *mce4* or *mce6X* mutants (Figure 4). If the rugose phenotype of the $omamA_{ms}$ mutant is due to the effective loss of Mce transport, the double $omamA_{ms}mce4$ and $omamA_{ms}mce6X$ should look like single *mce4* or *mce6X* mutants. If rugosity of the $omamA_{ms}$ mutant is independent of Mce transporter function, an additive effect on rugose morphology from losing both *mce* operons and $omamA_{ms}$ may occur. The double mutant phenotype was indistinguishable from that of the single mutants, suggesting that OmamA functions in the Mce transporter pathway.

OmamA is required for cholesterol utilization

The Mce4 transporter is the best characterized Mce system with a demonstrated function in cholesterol import. Mycobacterial mutants lacking the *mce4* operon are defective in cholesterol uptake and growth on cholesterol as a sole carbon source (Klepp *et al.*, 2012; Pandey & Sassetti, 2008). To test whether OmamA contributes to Mce4 function, we assayed the $omamA_{ms}$ mutant for its ability to utilize cholesterol as a sole carbon source. For these experiments, we followed the metabolic activity of mycobacteria using resazurin as previously described (Hayden *et al.*, 2013). Resazurin is a blue dye that converts to a pink fluorescent compound when reduced by metabolically active cells. *M. smegmatis* strains were grown in minimal media supplemented with standard glucose and glycerol carbon sources or cholesterol as the sole carbon source. In glucose and glycerol containing media,

both WT and the *omamA*$_{ms}$ mutant reduced resazurin over time (Figure 5A). However, in media with cholesterol as a sole carbon source, resazurin reduction was observed with WT *M. smegmatis* but the *omamA*$_{ms}$ mutant showed very little to no resazurin reduction. Strikingly, the behavior of the *omamA*$_{ms}$ mutant in cholesterol media was equivalent to that of the *mce4 M. smegmatis* mutant (Figure 5B). The cholesterol phenotype of the *omamA*$_{ms}$ mutant could be fully complemented by expression of either *omamA*$_{ms}$ or *omamA*$_{mtb}$ from a plasmid (Figure 5B).

To determine whether OmamA also contributes to Mce4 function in *M. tuberculosis*, we similarly tested the *M. tuberculosis omamA* mutant for a defect in utilization of cholesterol as a sole carbon source. *M. tuberculosis* transposon mutants in several *mce* operons, including the *mce4* operon (insertion mutants in the *mce4B* and *mce4F* genes), *mce1* (*mce1B*), and *mce2* (*mce2F*) were tested in parallel with the *omamA* mutant and complemented strains. In glycerol media, the *omamA* mutant behaved like WT in reducing resazurin over time (Figure 5C). However, in cholesterol media, the *omamA* mutant and *mce4* mutants with transposon insertions in *mce4B* or *mce4F* were unable to utilize cholesterol as a sole carbon source (Figure 5D). As with the *M. smegmatis* cholesterol experiments, the *omamA* and the *mce4* mutants of *M. tuberculosis* exhibited the same level of defect in cholesterol media. The *omamA* mutant was fully complemented by expression of *omamA*$_{mtb}$ in the complemented strain. Transposon mutants interrupting *mce1* and *mce2* operons displayed no defect for utilization of cholesterol (Figure 5D), consistent with previous reports (Pandey & Sassetti, 2008; Griffin *et al.*, 2011). These data demonstrate that OmamA is required for cholesterol utilization in both *M. smegmatis* and *M. tuberculosis*.

OmamA is required for cholesterol uptake

The cholesterol growth defects of *omamA* mutants of *M. smegmatis* or *M. tuberculosis* were indistinguishable from those of *mce4* mutants, suggesting a role of OmamA in Mce4 cholesterol import. To directly test whether OmamA is required for cholesterol import, as opposed to playing a role in downstream cholesterol metabolism, we tested the ability of WT *M. smegmatis*, the *omamA*$_{ms}$ mutant, and complemented strains to import radioactively labeled cholesterol. *M. smegmatis* strains were grown overnight in media with glucose and glycerol and then incubated for two hours in minimal media with C^{14} labeled cholesterol as the sole carbon source. After incubation, cells were washed extensively, and the level of accumulated cholesterol in the cells was quantified. In these experiments, the *mce4* mutant exhibited a two-fold reduction in cholesterol uptake in comparison to WT, consistent with previous reports (Pandey & Sassetti, 2008; Klepp *et al.*, 2012). The *omamA*$_{ms}$ mutant also revealed a defect in cholesterol uptake in comparison to WT, and this defect was equivalent to that observed with the *M. smegmatis mce4* mutant (Figure 6A). The cholesterol uptake defect of the *omamA* mutant could be complemented by either *omamA*$_{mtb}$ or *omamA*$_{ms}$ (Figure 6A). While both the *mce4* and *omamA*$_{ms}$ mutants exhibited a significant reduction in cholesterol uptake, there remained detectable levels of cell-associated C^{14} cholesterol with both mutants. Previous uptake studies also report residual levels of cholesterol associated with *mce4* mutants, leading to the suggestion that additional cholesterol importers may exist in mycobacteria (Pandey & Sassetti, 2008; Klepp *et al.*, 2012). When we examined the double *omamA*$_{ms}$*mce4* mutant it was no more defective than single *mce4* or

omamA$_{ms}$ mutants. In fact, the double mutant showed slightly improved cholesterol uptake in comparison to the single *mce4* and *omamA*$_{ms}$ mutations alone (Figure 6B). The lack of an additive effect of the *mce4* and *omamA*$_{ms}$ mutations on the cholesterol uptake phenotype is consistent with OmamA functioning in concert with Mce4 to import cholesterol, as opposed to being part of an independent cholesterol uptake pathway.

OmamA impacts the levels of Mce1 proteins

The above studies demonstrated that OmamA contributes to Mce4 cholesterol import and utilization. However, a function of OmamA beyond Mce4 seems likely. This is because the role of OmamA in promoting *M. tuberculosis* growth in resting murine macrophages (McCann *et al.*, 2011) cannot be explained by an effect on Mce4, as there is no obvious role for Mce4 in promoting growth in resting macrophages (Pandey & Sassetti, 2008; Stewart *et al.*, 2005; Rengarajan *et al.*, 2005; McCann *et al.*, 2011). However, because *M. tuberculosis mce1* mutantsare reported in several studies to be defective for growth in macrophages (Rengarajan *et al.*, 2005; Stewart *et al.*, 2005; McCann *et al.*, 2011), we hypothesized that OmamA contributes to Mce1 transporter function in addition to Mce4 function. Due to the predicted structural similarities between OmamA and VirB8, and the role of VirB8 in stabilizing the multi-protein type IV secretion complex (den Hartigh *et al.*, 2008; Sivanesan & Baron, 2011), we further hypothesized that OmamA stabilizes proteins within Mce transporter complexes. Thus, to investigate the potential contribution of OmamA to the Mce1 transporter system and stability of Mce complexes we performed Western blot analysis of four *M. tuberculosis* Mce1 proteins (Mce1A, Mce1D, Mce1E, and Mce1F) in *M. tuberculosis* WT, the *omamA* mutant, and the complemented strain. Mce1A, Mce1D, Mce1E, and Mce1F were localized to the cell wall in *M. tuberculosis* WT and the complemented strain, consistent with previous subcellular localization experiments performed in *M. smegmatis* (Forrellad *et al.*, 2014). However, Mce protein levels were dramatically diminished in the cell wall of the *omamA*$_{mtb}$ mutant (Figure 7A). Further, Mce1A, Mce1D, Mce1E, and Mce1F levels were significantly decreased in the whole cell lysate of the *omamA*$_{mtb}$ mutant, demonstrating that they were not merely mislocalized in the *omamA*$_{mtb}$ mutant. Mce1 protein levels were fully restored in the complemented strain. The effect of the *omamA* mutation on Mce proteins was not due to a broad defect on cell wall proteins, as shown by equivalent levels of the exported 19kD lipoprotein in cell wall fractions of all three strains (Figure 7A).

The Western blot results are consistent with Mce1 proteins being unstable in the absence of OmamA, however; an alternate explanation is that OmamA is required for the expression of genes in the *mce1* operon. To rule out the possibility that the dramatic reduction of Mce1 proteins in the *omamA* mutant is due to a transcriptional effect, we measured the level of *mce1* transcripts in WT, *omamA*$_{mtb}$ mutant, and complemented strains using Quantitative Real-Time PCR. All three strains harbored equivalent amounts of *mce1A* and *mce1F* transcripts. Thus, the dramatic decrease in of Mce1 protein levels in the *omamA* mutant is not a consequence of lower transcript levels. We similarly quantified *mce4* transcript levels in the *omamA*$_{mtb}$ mutant and again observed equivalent levels of *mce4A* and *mce4F* transcripts in the *omamA*$_{mtb}$ mutant compared to WT and complemented strains (Figure 7B).

Although the anti-Mce1D antibody was raised against a peptide from the *M. tuberculosis* protein, this antibody was also able to recognize the *M. smegmatis* Mce1D, which allowed us to similarly evaluate the level of Mce1D in the $omamA_{ms}$ mutant of *M. smegmatis.* The $omamA_{ms}$ mutant had less Mce1D protein in the whole cell lysate in comparison to WT or complemented strains while the level of GroEL2 protein, as a control, was equivalent across the three strains (Figure 7C). Thus, the effect of OmamA on Mce1 protein levels is observed in both *M. smegmatis* and *M. tuberculosis.*

OmamA stabilizes members of the Mce1 transport complex

The reduced levels of multiple Mce1 proteins in the *omamA* mutant is consistent with OmamA having a function, similar to that of VirB8, in stabilizing multi-component transporters. To more directly test for a role of OmamA in stabilizing Mce proteins, we added chloramphenicol to cultures of *M. tuberculosis* or *M. smegmatis omamA* mutant, WT and complemented strains to prevent new protein synthesis and then followed the decay of Mce proteins in whole cell lysates by Western blot. As expected from the previous experiments (Figure 7), in the *omamA* mutant of *M. tuberculosis* the level of Mce1A was reduced even prior to chloramphenicol treatment; however, by loading more protein, we were able to detect the protein and monitor its degradation. After 2 days of chloramphenicol treatment, Mce1A protein levels were unchanged in WT and complemented strains of *M. tuberculosis*. In contrast, Mce1A protein in the *omamA* mutant was highly unstable and over a two day time course the level of Mce1A was dramatically reduced (Figure 8A-B). The instability of Mce1A in the *omamA* mutant did not reflect general protein instability in our experimental conditions, as the exported 19 kD lipoprotein was equally stable in all three strains (Figure 8C-D). Similar experiments were performed in *M. smegmatis,* monitoring the stability of Mce1D. Following chloramphenicol addition, the level of Mce1D protein decreased at a faster rate in the $omamA_{ms}$ mutant than in the WT or complemented strains (Figure 8E), while degradation of a control protein, GroEL2, occurred at a similar rate in all strains (Figure 8F). Together, these data provide evidence for OmamA of *M. tuberculosis* and *M. smegmatis* playing a role in stabilizing components of the Mce1 transporter.

Discussion

The goal of this work was to extend our previous identification of OmamA as an exported protein of unknown function with a role in promoting growth in macrophages (McCann *et al.*, 2011). Here, we investigated the potential significance of similarities between OmamA and Mam proteins and we demonstrated a role for OmamA in cholesterol uptake, which is a Mce4 transporter-dependent process. We further showed that the contribution of OmamA to Mce transporters extends beyond Mce4 to Mce1, as revealed by the reduced levels and instability of Mce1 proteins in both *M. smegmatis* and *M. tuberculosis*. While our relatively limited understanding of the Mce1 transporter prevented us from more direct testing of an effect of OmamA on Mce1 function, the dramatic reduction in at least four Mce1 proteins in the *omamA* mutant of *M. tuberculosis* argues strongly for a role of OmamA in Mce1 transporter function, as is the case for Mce4. Our demonstration of a role of OmamA in Mce transporters is particularly striking given that the *omamA* gene is not linked to any *mce* operon and no Mam proteins have been functionally characterized previously. The lack of

assayable *in vitro* phenotypes similarly prevented us from testing a role for OmamA in the Mce2 and Mce3 systems. It remains a possibility that OmamA is also involved in these additional Mce transporter systems.

Both *M. smegmatis* and *M. tuberculosis* were used in this study. In particular, for logistical reasons, the cholesterol uptake experiment was performed in *M. smegmatis* as a model for *M. tuberculosis*. Although there is a risk that results may not translate between these species this seems unlikely to be the case here because the phenotypes of the *M. tuberculosis omamA* mutant are fully consistent with a role of OmamA in cholesterol uptake. In addition, our demonstration of *M. tuberculosis omamA* being able to complement the *M. smegmatis omamA* mutant phenotypes indicates conservation of function of the *M. smegmatis* and *M. tuberculosis* gene products.

Prior TraSH analysis predicted *omamA* to play a role during murine infection (Sassetti & Rubin, 2003; Zhang *et al.*, 2013). Our evaluation of mice infected with a single *omamA* mutant or a complemented strain in a low-dose aerosol model provides important validation of the TraSH prediction while also providing a more detailed picture of the contribution of *omamA* to *M. tuberculosis* infection. Our animal studies revealed the *omamA* mutant to have a reduced bacterial burden during the growth-*in-vivo* phase of infection (first 3 weeks), which is consistent with the role of OmamA in promoting *M. tuberculosis* growth in macrophages (McCann *et al.*, 2011). However, later in infection the organ burden of the mutant was no different than WT or complemented strains (as seen in independent experiments). Interestingly, despite the equalized bacterial burden later in infection the *omamA* mutant infected animals exhibited reduced pathology at late time points and prolonged survival compared to WT and complemented strains. It is worth noting that there are prior examples of *M. tuberculosis* mutants (i.e. *whiB3* and *sigH*) that elicit reduced immunopathology and prolonged survival of mice despite having a normal bacterial burden (Steyn *et al.*, 2002; Kaushal *et al.*, 2002). In these cases, the mutants are thought to be defective in the inducing harmful immunopathology, which could possibly be the case with the *omamA* mutant, as well. Alternatively, there may be long term consequences of the delayed growth phenotype of the *omamA* mutant that persist even after the bacterial burden catches up.

Because of the connection we made between OmamA and Mce systems, we compared the mouse phenotypes of the *omamA* mutant to infection phenotypes reported for *mce* mutants. Unfortunately, such comparisons are complicated by discrepant results between studies of *mce* mutants and the wide variety of models employed (infection route, single or pooled mutants, nature of the mutation, mouse strain, etc.) (Forrellad *et al.*, 2013; Casali & Riley, 2007). For *mce1* mutants, in particular, there are reports of attenuated as well as hypervirulent phenotypes (Gioffre *et al.*, 2005; Shimono *et al.*, 2003; Joshi *et al.*, 2006; Marjanovic *et al.*, 2010; Lima *et al.*, 2007; Sassetti & Rubin, 2003). Nonetheless, there are published reports of attenuated phenotypes of *mce1*, *mce2* and *mce3* mutants in mice that resemble those of the *omamA* mutant: reduced bacterial burden early in infection, increased survival time, and/or reduced lung pathology (Marjanovic *et al.*, 2010; Senaratne *et al.*, 2008; Sassetti & Rubin, 2003; Gioffre *et al.*, 2005; Joshi *et al.*, 2006). In contrast, *mce4* mutants are not reported to have defects early in infection but to have defects later during the

persistence phase, in particular when tested in an intravenous infection with a 1:1 mixture of WT:*mce4* strains (Joshi *et al.*, 2006; Pandey & Sassetti, 2008; Sassetti & Rubin, 2003). When tested in a single strain aerosol infection, similar to the one used in our study, a *mce4* mutant only exhibits a subtle defect in bacterial burden during the persistence phase of infection (Senaratne *et al.*, 2008), which may explain why we did not observe any defect in persistence. However, in the aerosol model reduced pathology late in infection and prolonged survival of mice infected with a *mce4* mutant is observed (Senaratne *et al.*, 2008). Thus, the *in vivo* growth defect of the *omamA* mutant is unlikely to result from an effect on Mce4, rather, a role of OmamA in additional Mce systems may account for this specific *in vivo* phenotype. However, future studies will be required to more clearly understand the *omamA* mutant phenotypes observed in animals.

The *omamA* mutant phenotypes we observed in cholesterol-containing media were indistinguishable from *mce4* mutants. These results not only support a role for OmamA in Mce4 transport, but they additionally reveal OmamA to be a new protein required for cholesterol utilization *in vitro*. In a Tn-seq mutagenesis study to identify *M. tuberculosis* genes required for *in vitro* growth on cholesterol, all genes in the *mce4* operon were identified, including *mam4A* and *mam4B*, but *omamA* was not identified (Griffin *et al.*, 2011). Interestingly, *omamA* barely missed the cutoff for statistical significance in this study (p=0.06), consistent with a role in cholesterol utilization.

It is also interesting to compare our results indicating a role for OmamA in Mce transport pathways to the results of a transposon mutagenesis screen conducted in *mce1* or *mce4* mutant backgrounds (Joshi *et al.*, 2006). In this genetic interaction screen, genes that are members of the same Mce transport pathway or genes in redundant parallel pathways were uncovered. Once again, although *omamA* was not predicted as having genetic interactions with *mce1* or *mce4* in this earlier study, inspection of the supplemental data revealed the behavior of *omamA* mutations in *mce1* and *mce4* backgrounds to be consistent with *omamA* being part of these Mce pathways (Joshi *et al.*, 2006).

Given the many *mce*-linked *mam* genes (eight) and unlinked *omam* (five) genes in *M. tuberculosis*, our finding that deletion of *omamA* yielded phenotypes as dramatic as complete deletion of the *mce4* operon was surprising, as was the discovery that OmamA impacted more than one Mce system. The dramatic phenotypes of the *omamA* mutant raise questions about whether other Mam proteins of *M. tuberculosis* will also have such broad effects. Data from transposon mutagenesis screens predicts similar phenotypes for mutations in *mam* genes and the adjoining *mce* operons (Rengarajan *et al.*, 2005; Sassetti & Rubin, 2003; Griffin *et al.*, 2011), which supports the idea of *mam* genes functioning with their linked *mce* system. It is possible that the function of *mce* operon associated *mam* genes may not extend to unlinked *mce* loci. For example, the *mce1*-associated *mam* genes (*mam1A-D*) are not predicted to be required for growth on cholesterol like *mce4* mutants (Griffin *et al.*, 2011). Furthermore, it remains unclear whether all orphaned Mam proteins are required for multiple Mce transporters or whether they are even involved in Mce transport at all. Individual *mam* and *omam* mutants will need to be constructed and characterized in order to determine if the dramatic role of OmamA in Mce function is unique or representative of the overall importance of all Mam family members.

The *Mycobacterium leprae* genome is highly reduced in comparison to other mycobacterial species and is thought to have only maintained a minimal set of genes required for its intracellular lifestyle (Moran, 2002; Singh & Cole, 2011). Interestingly, *omamA* and the downstream *omamB* are only two *omam* genes conserved in the *M. leprae* genome, which contains a single *mce* operon, *mce1* (Supplemental Figure 3). Conservation of *omamA* in *M. leprae* supports the importance of *omamA* in intracellular growth and virulence. Additionally, the conserved presence and arrangement of *omamA* and *omamB* suggests that the corresponding proteins may function together. Like *omamA* and *omamB*, Mam family proteins are usually encoded in pairs (Figure 1B, Supplemental Figure 3) (Casali & Riley, 2007), although the significance of this arrangement is unknown. Future study of OmamB, the protein encoded by *rv0200*, could help to determine whether OmamB also has a broad role in Mce transport like OmamA.

While crystal structures for Mam proteins will be necessary to prove structural similarity, the unexpected Phyre2 predictions were helpful for identifying a function for OmamA. VirB8 is an essential component of bacterial type IV secretion systems, with roles assembling the core complex of the transport machinery, providing stability to multiple proteins within the complex and potentially anchoring the transporter to the cytoplasmic membrane (Paschos *et al.*, 2006; Fronzes *et al.*, 2009; Kumar *et al.*, 2000; Baron, 2006). In the absence of VirB8, many proteins within the type IV secretion apparatus become destabilized and degraded (den Hartigh *et al.*, 2008; Sivanesan & Baron, 2011). Similarly, in the absence of OmamA all four of the *M. tuberculosis* Mce1 proteins and one *M. smegmatis* Mce1 protein we monitored were present at dramatically reduced levels. These reduced protein levels are due to protein instability, as shown by monitoring the stability of Mce1A in *M. tuberculosis* and Mce1D in *M. smegmatis*, as representative proteins. These results suggest that OmamA, and Mam proteins in general, may play analogous roles to VirB8 in the formation and stabilization of the core Mce1 transport complex, resulting in destabilization of the complex and individual Mce1 proteins in their absence. Due to a lack of anti-Mce4 antibodies, we were unable to test the effect of OmamA on the stability of proteins that comprise the Mce4 transporter. However, we propose that a similar function of OmamA in stabilization of the Mce4 transporter accounts for the defects in cholesterol uptake and metabolism observed in *omamA* mutants.

Interestingly, VirB8 also plays a role in substrate transport during type IV secretion (Cascales & Christie, 2004), which raises the possibility that Mam proteins may also have an additional role in Mce substrate movement. Due to structural and functional analogies between OmamA and VirB8, we propose a model wherein OmamA interacts with Mce proteins, potentially driving Mce complex formation and ultimately providing stability to Mce proteins within the complex (Figure 9). However, it is important to emphasize the speculative nature of the interactions depicted in this model, as there have yet to be any direct studies of protein-protein interactions in the presumed Mce macromolecular complex. Additionally, the stoichiometry of the proposed macromolecular complex remains unknown. Because there are thirteen Mam family proteins in *M. tuberculosis* and only four Mce transporters, we predict that each transporter may be stabilized by multiple Mam family members.

Although Mce transporters are of clear importance to *M. tuberculosis* virulence and a core component of the *M. tuberculosis* genome (Gioffre *et al.*, 2005; Shimono *et al.*, 2003; Marjanovic *et al.*, 2010; Lima *et al.*, 2007; Sassetti & Rubin, 2003; Rengarajan *et al.*, 2005; Stewart *et al.*, 2005; McCann *et al.*, 2011; Senaratne *et al.*, 2008; Pandey & Sassetti, 2008), there has yet to be a systematic genetic or biochemical analysis of the individual Mce transporter proteins in terms of their contribution to virulence or their function in the transport mechanism. Mce transporter components are assigned potential functions by analogy to classic ABC transporters (ex. ATPase, permease, or solute binding proteins) (Casali & Riley, 2007). However, Mce transporters are distinguished from ABC transporters in the multitude of individual proteins predicted to be involved: two YrbE permeases, six predicted Mce solute binding proteins, and a shared ATPase MceG. The function of all of these individual transporter components requires validation. Because Mam proteins share no obvious ABC transporter counterpart their function was an even bigger mystery. The results of this study provide an essential framework for studying the role of Mam family proteins in the stabilization of Mce transporter systems.

Experimental Procedures

Bacterial strains and plasmids

In this study, we used the bacterial strains listed in Supplemental Table 1 and plasmids as listed in Supplemental Table 2. The *M. tuberculosis omamA* (*rv0199*) mutant was generated in a previous transposon mutagenesis study performed in a *M. tuberculosis* β-lactamase (*ΔblaC*) background (McCann *et al.*, 2011; Flores *et al.*, 2005). The *omamA::tn* mutant has a hygromycin resistant Tn *'bla$_{TEM-1}$* transposon inserted in the *omamA* coding sequence at amino acid position 74 and it expresses an exported OmamA-'BlaTEM-1 fusion protein. The *omamA::tn* mutant (*omamA::tn, ΔblaC*) used in this study (MBTB319) additionally carries the empty pMV261.kan plasmid. For mutant characterization, *omamA::tn* was compared to strain MBTB178 (*omamA^{WT}, ΔblaC,* pJES137, pMV261.kan). Plasmid pJES137 is an integrating hygromycin resistant plasmid that expresses *'blaTEM-1.* MBTB178 is referred to as WT in the text. The *M. tuberculosis* complemented strain (*omamA::tn, ΔblaC,* pJES178) expresses *omamA* from the *hsp60* promoter of the kanamycin resistant plasmid pJES178 (McCann *et al.*, 2011). This series of *omamA::tn* (MBTB319), *omamA^{WT}* (MBTB178) and complemented (MBTB320) strains are all hygromycin and kanamycin resistant to enable growth in identical media conditions.

Bacterial growth

M. tuberculosis strains were grown in Middlebrook 7H9 broth (Difco) supplemented with 1X albumin dextrose saline (ADS), 0.5% glycerol and either 0.025% Tween 80 (Tw) or 0.025% tyloxapol (Ty). *M. smegmatis* strains were grown in Middlebrook 7H9 broth (Difco) supplemented with 0.2% glucose, 0.5% glycerol, and either 0.05% Tween 80 (Tw) or 0.05% Tyloxapol (Ty). Medium was supplemented with 20μg mL^{-1} kanamycin or 50μg mL^{-1} hygromycin as needed for mycobacterial cultures. *E. coli* strains were grown in Luria-Bertani medium (Fisher) supplemented as necessary with 40μg mL^{-1} kanamycin.

Mouse experiments

Female C57BL/6 mice aged 7-10 weeks were infected with ~200 cfu of *M. tuberculosis* by aerosol using a Madison chamber (Mechanical Engineering Workshop, Madison, WI), and bacterial burden was determined, as previously described (Kurtz *et al.*, 2006). Groups of four mice per strain were sacrificed, organs homogenized, and diluted and plated to determine bacterial burden at various times after infection. The lower right lobe of the lungs was inflated and fixed in 10% formalin for histology.

Histopathology

Inflammation was determined in 5 μm sections following hematoxylin and eosin (H&E) staining. Paraffin embedded sections were set and cut to reveal the maximum longitudinal visualization of the intrapulmonary main axial airway. Histopathology was evaluated and scored by an experienced blinded reviewer (I.C.A.) on a scale of 0 (absent) to 3 (severe), as previously described (McElvania Tekippe *et al.*, 2010; Allen *et al.*, 2013; Allen *et al.*, 2009). The parameters assessed included overall leukocyte infiltration, perivascular and peribroncheolar cuffing, extravasation, and the estimated percent of lung area involved with inflammation. Each individual parameter was scored and averaged to generate the histology score.

Mutant construction

M. smegmatis mutants were constructed by recombineering, as previously described (van Kessel & Hatfull, 2008; van Kessel & Hatfull, 2007). Briefly, upstream and downstream flanks were PCR amplified and cloned into pMP614 (kind gift from Martin Pavelka), which was then linearized to produce the final recombineering fragment, carrying a hygromycin resistance marker flanked by DNA sequences upstream and downstream of *msmeg0235*. Parental strains carrying a kanamycin marked plasmid expressing a recombinase, pJV53, (van Kessel & Hatfull, 2007; van Kessel & Hatfull, 2008) were used for recombineering. Following three hour induction of the recombinase with acetamide, electroporation was used to introduce the linear recombineering fragment. Allelic exchange recombinants were selected for double resistance to hygromycin and kanamycin. Strains were cured of pJV53 by passaging 3-4 times in the absence of kanamycin. Plasmid cured strains were then transformed with the resolvase expressing pMP854 plasmid (kind gift from Martin Pavelka), to remove the hygromycin marker in the deletion cassette. Hyg^s strains were cured for pMP854 as described above to generate the final unmarked deletion strains. Mutant construction was confirmed by Southern blot (data not shown).

$OmamA_{ms}$ complementation and $OmamA_{mtb}$-HA vector construction

The *msmeg0235* gene ($omamA_{ms}$) was PCR amplified by *msmeg0235*_F1 x *msmeg0235*_R1, the *rv0199* gene ($omamA_{mtb}$) was PCR amplified by *rv0199HA*_F_MscI x *rv0199HA*_R_HindIII, and PCR fragments were cloned into pCR2.1 (Invitrogen). The resulting plasmids were sequenced to confirm they were error-free. The $omamA_{ms}$ fragment was digested from pCR2.1 with EcoRI, gel purified, and ligated into EcoRI digested pMV261.kan (Stover *et al.*, 1991). The $omamA_{mtb}$ fragment was digested from pCR2.1 with MscI and HindIII, gel purified, and ligated into MscI/HindIII digested JSC77 (Glickman *et*

al., 2000), containing an in-frame C-terminal HA tag. Primer sequences are provided (Supplemental Table 3).

Transformation

M. smegmatis strains were transformed by electroporation, as previously described (Snapper *et al.*, 1990).

Morphology

Congo red assays were performed, as previously described (Klepp *et al.*, 2012). Mueller Hinton agar plates were supplemented with 0.2% glucose and 100μg mL^{-1} Congo red (Sigma). Colony morphology was analyzed by plating 2 μL spots of OD_{600} 1.0 *M. smegmatis* strains. Plates were incubated at 37°C for two days and visualized using a low-magnification Leica M420 macroscope with 2X and 5.6X magnification.

Cholesterol Metabolism Assays for M. tuberculosis

A cholesterol stock solution was prepared by solubilizing cholesterol in ethanol and tyloxapol, as follows. A 1:1 solution of 200 proof ethanol:Tyloxapol (Sigma) was prepared, filtered, and heated to 50°C. 200mg mL^{-1} cholesterol was dissolved in 3:1 chloroform:methanol, and added dropwise to the 50°C tyloxapol solution until reaching 20% final volume. Sauton's media was prepared and pH adjusted to 7.4: 1L dH_2O, 4g DL asparagine, 2g sodium citrate, 0.5g K_2HPO_4, 0.5g $MgSO_4$-$7H_2O$, 0.05g ferric ammonium citrate, 0.025% Tyloxapol, and supplemented with either 6% glycerol or 0.5 mM cholesterol from stock solution. *M. tuberculosis* strains were diluted to 10^5 cfu mL^{-1} in Sauton's +Ty and 10^4 cfu were aliquoted into 96 well plates with Sauton's supplemented with glycerol or cholesterol, incubated shaking at 37°C for seven days, then resazurin (Sigma) was added to a final concentration 0.0125 mg mL^{-1}. Resazurin conversion was followed using fluorescence and was monitored daily by a Tecan Infinite 200 Pro at hv=544 nm excitation and hv=590 nm emission.

Cholesterol Metabolism Assays for M. smegmatis

A cholesterol stock solution was prepared by solubilizing cholesterol in cyclodextrin, as previously described (Klein *et al.*, 1995). Briefly, 1g methyl-ß-cyclodextrin (C4555 Sigma) was dissolved in 11mL PBS (0.09g mL^{-1}) and heated to 80°C with continuous stirring. 30 mg cholesterol (Sigma) was dissolved in 400μL 2:1 isopropanol/chloroform. The cholesterol solution was added to the cyclodextrin in 50μL aliquots, stirring continuously. The solution was cooled slowly, filtered for sterility, and kept at room temperature. M9 minimal media was prepared as follows: 1L dH_2O, 12.8g Na_2HPO_4, 3g KH_2PO_4, 0.5g NaCl, 1g NH_4Cl, 25 μL 1M $CaCl_2$, 500μL 1M $MgSO_4$, and 2.5 mL 10% Tyloxapol (Ty, Sigma), and supplemented with 0.2% glucose and 0.5% glycerol or 0.5mM cholesterol from stock solution. *M. smegmatis* strains were grown to OD_{600} 1.0 in M9 supplemented with 0.2% glucose and 0.5% glycerol + 0.05% Ty. Strains were washed in M9 +Ty three times by pelleting cells at 1,900 × *g* for 10 minutes at 4°C, and diluted to 10^5 cfu mL^{-1} in M9 +Ty, and 10^4 cfu were plated into 96 well plates with M9 containing glycerol or cholesterol. Plates were incubated shaking at 37°C overnight, after which resazurin (Sigma) was added

to a final concentration 0.0125 mg mL^{-1}. Florescence was monitored every 10 minutes by a Spectramax M2 using hv=544 nm excitation and hv=590 nm emission.

Cholesterol uptake

Cholesterol uptake experiments were performed, similar to previously reported (Klepp *et al.*, 2012). *M. smegmatis* strains were grown to OD_{600} 1.0 in M9 supplemented with 0.2% glucose and 0.5% glycerol + 0.05% Ty. Strains were washed in M9 + Ty three times by pelleting cells at 1,900 × *g* for 10 minutes at 4°C, and then equalized to OD_{600} 0.5 in M9 + Ty, and incubated with 0.04μCi 4-C^{14} cholesterol (Perkin Elmer NEC018050UC) for 2 hours at 37°C. After incubation, cells were pelleted and washed three times with M9 + Ty, and cell associated radioactivity was measured by scintillation counter.

Subcellular fractionation

M. tuberculosis cells were pelleted by centrifugation (1,900 × *g*) and sterilized by irradiation (JL Shephard Mark I 137Cs irradiator, Department of Radiobiology, University of North Carolina at Chapel Hill). After sterilization, *M. tuberculosis* cells were removed from BSL-3 containment. *M. smegmatis* cells were simply pelleted by centrifugation for 10 minutes at 1,900 × *g*. Subcellular fractionation was then performed, as previously described (Gibbons *et al.*, 2007). Briefly, cells were resuspended in PBS containing protease inhibitors, lysed in a French pressure cell, and unlysed cells were removed by centrifugation (1,900 × *g*). The clarified whole cell lysates (WCL) were subjected to differential ultracentrifugation, 27,000 × *g* for 30 minutes to pellet the cell wall (CW), 100,000 × *g* for 2 hours to pellet the membrane (MEM), and remaining soluble (SOL) fraction containing the cytoplasm.

Western blotting

Equal protein amounts, as determined by Bicinchonic acid assay (Pierce), for all fractions and strains were separated by SDS-PAGE and transferred to nitrocellulose membranes. Proteins were detected using the following antibodies: Mce1 antibodies (a gift from Christopher Sassetti, University of Massachusetts Medical School (Feltcher *et al.*, 2015)): anti-Mce1A (1:10,000), anti-Mce1D (1:5,000), anti-Mce1E/Lprk (1:5,000), anti-Mce1F (1:10,000), anti-19kD (1:20,000) (a gift from Douglas Young, Imperial College, United Kingdom), and anti-HA (1:25,000) (Covance). GroEL2 was detected using an anti-HIS (1:10,000) (Abgent) antibody, as previously described (Feltcher *et al.*, 2013), which recognizes a string of histidines in GroEL2 (Rengarajan *et al.*, 2008). Anti-mouse and Anti-rabbit IgG conjugated HRP (Biorad) were used as secondary antibodies, as appropriate. HRP signal was detected using Western Lighting Chemiluminescent detection reagent (Perkin-Elmer). Quantitation of Western blots was calculated by densitometry using ImageJ (Schneider *et al.*, 2012).

Quantitative Real-Time PCR

Triplicate *M. tuberculosis* cultures were grown to OD_{600} of 1.0 and pelleted by centrifugation for 10 minutes at 1,900 × *g*, and qRT-PCR was performed. Bacteria were lysed by 3:1 chloroform methanol, mixed with Trizol (Invitrogen), and the upper phase was separated and RNA precipitated overnight in isopropanol. RNA samples were pelleted and

washed in 70% ethanol, and resuspended in RNase-free H_2O. RNA samples were treated with DNase (Promega), purified (Zymo RNA Clean and Concentrator Kit), and converted to cDNA using iScript cDNA Synthesis Kit (BioRad). Triplicate biological and triplicate technical replicates of cDNA from 40 ng RNA each were used for qRT-PCR using the Sensimix SYBR and Flourescein kit (Bioline). Transcript copy number for each gene was calculated as compared to known concentrations of genomic DNA, and each sample was normalized to housekeeping gene *sigA* transcript levels. Primer sequences are provided (Supplemental Table 3).

Protein stability experiments

Cultures of *M. tuberculosis* or *M. smegmatis* were first grown to approximately OD_{600} 1.0 and diluted to OD_{600} 0.5 in media containing 20 ug mL^{-1} or 35 ug mL^{-1} of chloramphenicol (Sigma) for *M. tuberculosis* and *M. smegmatis*, respectively. At specific time points, samples were taken to measure the amount of Mce1 protein present in WCL. For *M. tuberculosis* samples, prior to cell lysis the cells were washed twice with PBS + 0.02% Tween 80, sterilized by fixation in an equal volume of 10% formalin (Fisher) for 1 hour and washed post-fixation. Whole cell lysates were prepared as previously described (Braunstein *et al.*, 2001). Briefly, cells were resuspended in extraction buffer, lysed by MagNA Lyser (Roche) with glass beads, and denatured by boiling. Equal protein amounts as determined by Bicinchonic acid assay (Pierce) were loaded for Western blot analysis, as described above. Quantitation of Western blots was calculated by densitometry using ImageJ (Schneider *et al.*, 2012).

Statistics

Statistics were performed in SigmaPlot. Normality testing (Shapiro-Wilk) and equal variance testing was done to determine correct statistical methods. Comparisons passing normality and equal variance with two groups were performed by two-tailed Student's t-test. Comparisons not passing normality with two groups were performed by Mann-Whitney rank sum test. Comparisons passing normality and equal variance with more than two groups used one way analysis of variance (ANOVA), followed by multiple comparisons with the Holm-Sidak method as appropriate. Comparisons not passing normality with more than two groups used Kruskal-Wallis one way analysis of variance on ranks, followed by multiple comparisons with Student-Newman-Keuls. Survival was analyzed by Log-rank test followed by multiple comparisons with the Holm-Sidak method.

Supplementary Material

Refer to Web version on PubMed Central for supplementary material.

Acknowledgements

This work was supported by a Burroughs Wellcome Investigator in Pathogenesis of Infectious Disease Award, by NIH R21 AI076685 and NIH RO1 AI054540 Awards (to M.B.). E.F.P. was supported by a University of North Carolina Dissertation Completion Fellowship. J.R.M. was supported by training grant NIH 5-T32-GM008581 and a Society of Fellows graduate dissertation fellowship. J.T.S. was supported by a University of North Carolina Morehead Fellowship.

We would like to thank Sara Johnson for assistance with this work. We would like to thank Fabiana Bigi for providing the *mce4* and *mce6X M. smegmatis* strains, Chris Sassetti and Jennifer Griffin for providing the Mce1 antibodies, and Douglas Young for providing the 19kD antibody. We would like to thank Martin Pavelka for providing the plasmids pMP614 and pMP854. We also thank Peggy Cotter, Mary Hondalus and all members of the Braunstein lab for critical reading of the manuscript.

References

Allen IC, McElvania-TeKippe E, Wilson JE, Lich JD, Arthur JC, Sullivan JT, Braunstein M, Ting JP. Characterization of NLRP12 during the *in vivo* host immune response to *Klebsiella pneumoniae* and *Mycobacterium tuberculosis*. PLoS One. 2013; 8:e60842. [PubMed: 23577168]

Allen IC, Scull MA, Moore CB, Holl EK, McElvania-TeKippe E, Taxman DJ, Guthrie EH, Pickles RJ, Ting JP. The NLRP3 inflammasome mediates in vivo innate immunity to influenza A virus through recognition of viral RNA. Immunity. 2009; 30:556–565. [PubMed: 19362020]

Altschul SF, Gish W, Miller W, Myers EW, Lipman DJ. Basic local alignment search tool. J Mol Biol. 1990; 215:403–410. [PubMed: 2231712]

Bailey S, Ward D, Middleton R, Grossmann JG, Zambryski PC. *Agrobacterium tumefaciens* VirB8 structure reveals potential protein-protein interaction sites. Proc Natl Acad Sci U S A. 2006; 103:2582–2587. [PubMed: 16481621]

Baron C. VirB8: a conserved type IV secretion system assembly factor and drug target. Biochemistry and cell biology = Biochimie et biologie cellulaire. 2006; 84:890–899. [PubMed: 17215876]

Braunstein M, Brown AM, Kurtz S, Jacobs WR Jr. Two nonredundant SecA homologues function in mycobacteria. J Bacteriol. 2001; 183:6979–6990. [PubMed: 11717254]

Briken V. *Mycobacterium tuberculosis* genes involved in regulation of host cell death. Adv Exp Med Biol. 2013; 783:93–102. [PubMed: 23468105]

Cantrell SA, Leavell MD, Marjanovic O, Iavarone AT, Leary JA, Riley LW. Free mycolic acid accumulation in the cell wall of the *mce1* operon mutant strain of *Mycobacterium tuberculosis*. Journal of microbiology. 2013; 51:619–626.

Casali N, Riley LW. A phylogenomic analysis of the Actinomycetales mce operons. BMC Genomics. 2007; 8:60. [PubMed: 17324287]

Cascales E, Christie PJ. Definition of a bacterial type IV secretion pathway for a DNA substrate. Science. 2004; 304:1170–1173. [PubMed: 15155952]

Chaillan-Huntington C, Butler PJ, Huntington JA, Akin D, Feldherr C, Stewart M. NTF2 monomer-dimer equilibrium. J Mol Biol. 2001; 314:465–477. [PubMed: 11846560]

Darwin KH, Ehrt S, Gutierrez-Ramos JC, Weich N, Nathan CF. The proteasome of *Mycobacterium tuberculosis* is required for resistance to nitric oxide. Science. 2003; 302:1963–1966. [PubMed: 14671303]

den Hartigh AB, Rolan HG, de Jong MF, Tsolis RM. VirB3 to VirB6 and VirB8 to VirB11, but not VirB7, are essential for mediating persistence of Brucella in the reticuloendothelial system. J Bacteriol. 2008; 190:4427–4436. [PubMed: 18469100]

Deretic V. Autophagy, an immunologic magic bullet: *Mycobacterium tuberculosis* phagosome maturation block and how to bypass it. Future Microbiol. 2008; 3:517–524. [PubMed: 18811236]

Feltcher ME, Gibbons HS, Ligon LS, Braunstein M. Protein export by the mycobacterial SecA2 system is determined by the preprotein mature domain. J Bacteriol. 2013; 195:672–681. [PubMed: 23204463]

Feltcher ME, Gunawardena HP, Zulauf KE, Malik S, Griffin JE, Sassetti CM, Chen X, Braunstein M. Label-free quantitative proteomics reveals a role for the *Mycobacterium tuberculosis* SecA2 pathway in exporting solute binding proteins and Mce transporters to the cell wall. Molecular & cellular proteomics : MCP. 2015

Flores AR, Parsons LM, Pavelka MS Jr. Genetic analysis of the beta-lactamases of *Mycobacterium tuberculosis* and *Mycobacterium smegmatis* and susceptibility to beta-lactam antibiotics. Microbiology. 2005; 151:521–532. [PubMed: 15699201]

Forrellad MA, Klepp LI, Gioffre A, Sabio y Garcia J, Morbidoni HR, de la Paz Santangelo M, Cataldi AA, Bigi F. Virulence factors of the *Mycobacterium tuberculosis* complex. Virulence. 2013; 4:3–66. [PubMed: 23076359]

Forrellad MA, McNeil M, Santangelo Mde L, Blanco FC, Garcia E, Klepp LI, Huff J, Niederweis M, Jackson M, Bigi F. Role of the Mce1 transporter in the lipid homeostasis of *Mycobacterium tuberculosis*. Tuberculosis (Edinb). 2014; 94:170–177. [PubMed: 24440549]

Fronzes R, Christie PJ, Waksman G. The structural biology of type IV secretion systems. Nat Rev Microbiol. 2009; 7:703–714. [PubMed: 19756009]

Gibbons HS, Wolschendorf F, Abshire M, Niederweis M, Braunstein M. Identification of two *Mycobacterium smegmatis* lipoproteins exported by a SecA2-dependent pathway. J Bacteriol. 2007; 189:5090–5100. [PubMed: 17496088]

Gioffre A, Infante E, Aguilar D, Santangelo MP, Klepp L, Amadio A, Meikle V, Etchechoury I, Romano MI, Cataldi A, Hernandez RP, Bigi F. Mutation in mce operons attenuates *Mycobacterium tuberculosis* virulence. Microbes Infect. 2005; 7:325–334. [PubMed: 15804490]

Glickman MS, Cox JS, Jacobs WR Jr. A novel mycolic acid cyclopropane synthetase is required for cording, persistence, and virulence of *Mycobacterium tuberculosis*. Mol Cell. 2000; 5:717–727. [PubMed: 10882107]

Goujon M, McWilliam H, Li W, Valentin F, Squizzato S, Paern J, Lopez R. A new bioinformatics analysis tools framework at EMBL-EBI. Nucleic Acids Res. 2010; 38:W695–699. [PubMed: 20439314]

Griffin JE, Gawronski JD, Dejesus MA, Ioerger TR, Akerley BJ, Sassetti CM. High-resolution phenotypic profiling defines genes essential for mycobacterial growth and cholesterol catabolism. PLoS Pathog. 2011; 7:e1002251. [PubMed: 21980284]

Hayden JD, Brown LR, Gunawardena HP, Perkowski EF, Chen X, Braunstein M. Reversible acetylation regulates acetate and propionate metabolism in *Mycobacterium smegmatis*. Microbiology. 2013; 159:1986–1999. [PubMed: 23813678]

Hicks SW, Galan JE. Exploitation of eukaryotic subcellular targeting mechanisms by bacterial effectors. Nat Rev Microbiol. 2013; 11:316–326. [PubMed: 23588250]

Hinchey J, Lee S, Jeon BY, Basaraba RJ, Venkataswamy MM, Chen B, Chan J, Braunstein M, Orme IM, Derrick SC, Morris SL, Jacobs WR Jr. Porcelli SA. Enhanced priming of adaptive immunity by a proapoptotic mutant of *Mycobacterium tuberculosis*. The Journal of clinical investigation. 2007; 117:2279–2288. [PubMed: 17671656]

Isaac DT, Isberg R. Master manipulators: an update on Legionella pneumophila Icm/Dot translocated substrates and their host targets. Future Microbiol. 2014; 9:343–359. [PubMed: 24762308]

Joshi SM, Pandey AK, Capite N, Fortune SM, Rubin EJ, Sassetti CM. Characterization of mycobacterial virulence genes through genetic interaction mapping. Proc Natl Acad Sci U S A. 2006; 103:11760–11765. [PubMed: 16868085]

Kaushal D, Schroeder BG, Tyagi S, Yoshimatsu T, Scott C, Ko C, Carpenter L, Mehrotra J, Manabe YC, Fleischmann RD, Bishai WR. Reduced immunopathology and mortality despite tissue persistence in a *Mycobacterium tuberculosis* mutant lacking alternative sigma factor, SigH. Proc Natl Acad Sci U S A. 2002; 99:8330–8335. [PubMed: 12060776]

Kelley LA, Sternberg MJ. Protein structure prediction on the Web: a case study using the Phyre server. Nat Protoc. 2009; 4:363–371. [PubMed: 19247286]

Klein U, Gimpl G, Fahrenholz F. Alteration of the myometrial plasma membrane cholesterol content with beta-cyclodextrin modulates the binding affinity of the oxytocin receptor. Biochemistry. 1995; 34:13784–13793. [PubMed: 7577971]

Klepp LI, Forrellad MA, Osella AV, Blanco FC, Stella EJ, Bianco MV, Santangelo Mde L, Sassetti C, Jackson M, Cataldi AA, Bigi F, Morbidoni HR. Impact of the deletion of the six mce operons in *Mycobacterium smegmatis*. Microbes Infect. 2012; 14:590–599. [PubMed: 22353253]

Krogh A, Larsson B, von Heijne G, Sonnhammer EL. Predicting transmembrane protein topology with a hidden Markov model: application to complete genomes. J Mol Biol. 2001; 305:567–580. [PubMed: 11152613]

Kumar RB, Xie YH, Das A. Subcellular localization of the *Agrobacterium tumefaciens* TDNA transport pore proteins: VirB8 is essential for the assembly of the transport pore. Mol Microbiol. 2000; 36:608–617. [PubMed: 10844650]

Kuroda T, Kubori T, Thanh Bui X, Hyakutake A, Uchida Y, Imada K, Nagai H. Molecular and structural analysis of Legionella DotI gives insights into an inner membrane complex essential for type IV secretion. Scientific reports. 2015; 5:10912. [PubMed: 26039110]

Kurtz S, McKinnon KP, Runge MS, Ting JP, Braunstein M. The SecA2 secretion factor of *Mycobacterium tuberculosis* promotes growth in macrophages and inhibits the host immune response. Infect Immun. 2006

Lew JM, Kapopoulou A, Jones LM, Cole ST. TubercuList--10 years after. Tuberculosis (Edinb). 2011; 91:1–7. [PubMed: 20980199]

Ligon LS, Hayden JD, Braunstein M. The ins and outs of *Mycobacterium tuberculosis* protein export. Tuberculosis (Edinb). 2012; 92:121–132. [PubMed: 22192870]

Lima P, Sidders B, Morici L, Reader R, Senaratne R, Casali N, Riley LW. Enhanced mortality despite control of lung infection in mice aerogenically infected with a *Mycobacterium tuberculosis* mce1 operon mutant. Microbes Infect. 2007; 9:1285–1290. [PubMed: 17890119]

Manganelli R, Dubnau E, Tyagi S, Kramer FR, Smith I. Differential expression of 10 sigma factor genes in *Mycobacterium tuberculosis*. Mol Microbiol. 1999; 31:715–724. [PubMed: 10027986]

Manzanillo PS, Shiloh MU, Portnoy DA, Cox JS. *Mycobacterium tuberculosis* activates the DNA-dependent cytosolic surveillance pathway within macrophages. Cell Host Microbe. 2012; 11:469–480. [PubMed: 22607800]

Marjanovic O, Miyata T, Goodridge A, Kendall LV, Riley LW. Mce2 operon mutant strain of *Mycobacterium tuberculosis* is attenuated in C57BL/6 mice. Tuberculosis (Edinb). 2010; 90:50–56. [PubMed: 19963438]

Marmiesse M, Brodin P, Buchrieser C, Gutierrez C, Simoes N, Vincent V, Glaser P, Cole ST, Brosch R. Macro-array and bioinformatic analyses reveal mycobacterial 'core' genes, variation in the ESAT-6 gene family and new phylogenetic markers for the *Mycobacterium tuberculosis* complex. Microbiology. 2004; 150:483–496. [PubMed: 14766927]

McCann JR, McDonough JA, Sullivan JT, Feltcher ME, Braunstein M. Genome-wide identification of *Mycobacterium tuberculosis* exported proteins with roles in intracellular growth. J Bacteriol. 2011; 193:854–861. [PubMed: 21148733]

McCann, JR.; Kurtz, S.; Braunstein, M. Secreted and exported proteins important to *Mycobacterium tuberculosis* pathogenesis.. In: Wooldridge, K., editor. Bacterial Secreted Proteins: Secretory Mechanisms and Role in Pathogenesis. Caister Academic Press; Norfolk, UK: 2009. p. 265-298.

McElvania Tekippe E, Allen IC, Hulseberg PD, Sullivan JT, McCann JR, Sandor M, Braunstein M, Ting JP. Granuloma formation and host defense in chronic *Mycobacterium tuberculosis* infection requires PYCARD/ASC but not NLRP3 or caspase-1. PLoS One. 2010; 5:e12320. [PubMed: 20808838]

Mohn WW, van der Geize R, Stewart GR, Okamoto S, Liu J, Dijkhuizen L, Eltis LD. The actinobacterial mce4 locus encodes a steroid transporter. J Biol Chem. 2008; 283:35368–35374. [PubMed: 18955493]

Moran NA. Microbial minimalism: genome reduction in bacterial pathogens. Cell. 2002; 108:583–586. [PubMed: 11893328]

Niederweis M. Nutrient acquisition by mycobacteria. Microbiology. 2008; 154:679–692. [PubMed: 18310015]

Pandey AK, Sassetti CM. Mycobacterial persistence requires the utilization of host cholesterol. Proc Natl Acad Sci U S A. 2008; 105:4376–4380. [PubMed: 18334639]

Paschos A, Patey G, Sivanesan D, Gao C, Bayliss R, Waksman G, O'Callaghan D, Baron C. Dimerization and interactions of Brucella suis VirB8 with VirB4 and VirB10 are required for its biological activity. Proc Natl Acad Sci U S A. 2006; 103:7252–7257. [PubMed: 16648257]

Rengarajan J, Bloom BR, Rubin EJ. Genome-wide requirements for *Mycobacterium tuberculosis* adaptation and survival in macrophages. Proc Natl Acad Sci U S A. 2005; 102:8327–8332. [PubMed: 15928073]

Rengarajan J, Murphy E, Park A, Krone CL, Hett EC, Bloom BR, Glimcher LH, Rubin EJ. *Mycobacterium tuberculosis* Rv2224c modulates innate immune responses. Proc Natl Acad Sci U S A. 2008; 105:264–269. [PubMed: 18172199]

Sassetti CM, Rubin EJ. Genetic requirements for mycobacterial survival during infection. Proc Natl Acad Sci U S A. 2003; 100:12989–12994. [PubMed: 14569030]

Schneider CA, Rasband WS, Eliceiri KW. NIH Image to ImageJ: 25 years of image analysis. Nature methods. 2012; 9:671–675. [PubMed: 22930834]

Senaratne RH, Sidders B, Sequeira P, Saunders G, Dunphy K, Marjanovic O, Reader JR, Lima P, Chan S, Kendall S, McFadden J, Riley LW. *Mycobacterium tuberculosis* strains disrupted in mce3 and mce4 operons are attenuated in mice. Journal of medical microbiology. 2008; 57:164–170. [PubMed: 18201981]

Shimono N, Morici L, Casali N, Cantrell S, Sidders B, Ehrt S, Riley LW. Hypervirulent mutant of *Mycobacterium tuberculosis* resulting from disruption of the mce1 operon. Proc Natl Acad Sci U S A. 2003; 100:15918–15923. [PubMed: 14663145]

Simeone R, Sayes F, Song O, Groschel MI, Brodin P, Brosch R, Majlessi L. Cytosolic access of *Mycobacterium tuberculosis*: critical impact of phagosomal acidification control and demonstration of occurrence in vivo. PLoS Pathog. 2015; 11:e1004650. [PubMed: 25658322]

Singh P, Cole ST. Mycobacterium leprae: genes, pseudogenes and genetic diversity. Future Microbiol. 2011; 6:57–71. [PubMed: 21162636]

Sivanesan D, Baron C. The dimer interface of *Agrobacterium tumefaciens* VirB8 is important for type IV secretion system function, stability, and association of VirB2 with the core complex. J Bacteriol. 2011; 193:2097–2106. [PubMed: 21398549]

Smith MA, Coincon M, Paschos A, Jolicoeur B, Lavallee P, Sygusch J, Baron C. Identification of the binding site of Brucella VirB8 interaction inhibitors. Chem Biol. 2012; 19:1041–1048. [PubMed: 22921071]

Snapper SB, Melton RE, Mustafa S, Kieser T, Jacobs WR Jr. Isolation and characterization of efficient plasmid transformation mutants of *Mycobacterium smegmatis*. Mol Microbiol. 1990; 4:1911–1919. [PubMed: 2082148]

Stewart GR, Patel J, Robertson BD, Rae A, Young DB. Mycobacterial mutants with defective control of phagosomal acidification. PLoS Pathog. 2005; 1:269–278. [PubMed: 16322769]

Steyn AJ, Collins DM, Hondalus MK, Jacobs WR Jr. Kawakami RP, Bloom BR. *Mycobacterium tuberculosis* WhiB3 interacts with RpoV to affect host survival but is dispensable for in vivo growth. Proc Natl Acad Sci U S A. 2002; 99:3147–3152. [PubMed: 11880648]

Stover CK, de la Cruz VF, Fuerst TR, Burlein JE, Benson LA, Bennett LT, Bansal GP, Young JF, Lee MH, Hatfull GF. New use of BCG for recombinant vaccines. Nature. 1991; 351:456–460. [PubMed: 1904554]

Sturgill-Koszycki S, Schlesinger PH, Chakraborty P, Haddix PL, Collins HL, Fok AK, Allen RD, Gluck SL, Heuser J, Russell DG. Lack of acidification in Mycobacterium phagosomes produced by exclusion of the vesicular proton-ATPase. Science. 1994; 263:678–681. [PubMed: 8303277]

Terradot L, Bayliss R, Oomen C, Leonard GA, Baron C, Waksman G. Structures of two core subunits of the bacterial type IV secretion system, VirB8 from Brucella suis and ComB10 from Helicobacter pylori. Proc Natl Acad Sci U S A. 2005; 102:4596–4601. [PubMed: 15764702]

Thompson JD, Gibson TJ, Higgins DG. Multiple sequence alignment using ClustalW and ClustalX. Current protocols in bioinformatics / editoral board, Andreas D. Baxevanis ... [et al.]. 2002 Chapter 2: Unit 2 3.

van der Wel N, Hava D, Houben D, Fluitsma D, van Zon M, Pierson J, Brenner M, Peters PJ. M. tuberculosis and M. leprae translocate from the phagolysosome to the cytosol in myeloid cells. Cell. 2007; 129:1287–1298. [PubMed: 17604718]

van Kessel JC, Hatfull GF. Recombineering in *Mycobacterium tuberculosis*. Nature methods. 2007; 4:147–152. [PubMed: 17179933]

van Kessel JC, Hatfull GF. Mycobacterial recombineering. Methods Mol Biol. 2008; 435:203–215. [PubMed: 18370078]

World Health Organization. Global Tuberculosis Report 2014. 2014

Zhang YJ, Reddy MC, Ioerger TR, Rothchild AC, Dartois V, Schuster BM, Trauner A, Wallis D, Galaviz S, Huttenhower C, Sacchettini JC, Behar SM, Rubin EJ. Tryptophan biosynthesis protects mycobacteria from CD4 T-cell-mediated killing. Cell. 2013; 155:1296–1308. [PubMed: 24315099]

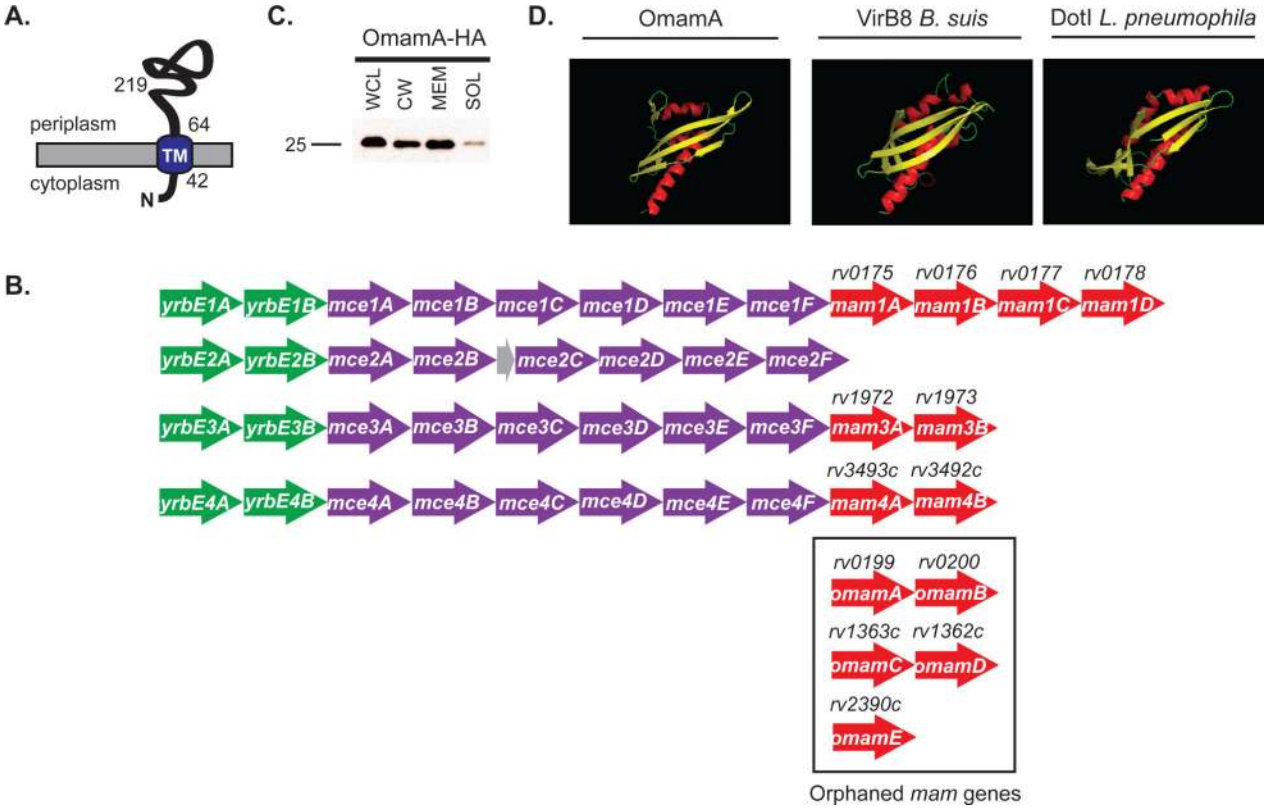

Figure 1.

Rv0199 (OmamA) is a transmembrane protein predicted to be a Mce-associated protein. **A.** OmamA is predicted to have a single N-terminal transmembrane domain (TM) at amino acid 42-64 (Krogh *et al.*, 2001) and C-terminal domain exposed to the cell wall side of the membrane (McCann *et al.*, 2011). **B.** OmamA is predicted to be a Mce-associated membrane (Mam) protein, however, *rv0199* is not located in a *mce* operon. *Mce* operons are typically organized by two *yrbE* genes upstream (green), six *mce* genes (purple) and most have pairs of *mam* genes (red) downstream. Genes encoding putative orphaned *mam* genes are boxed. Genes encoding Omam proteins are distinguished by being distally located from *mce* operons (Casali & Riley, 2007). The *mce2* operon additionally contains a small predicted pseudogene (grey). **C.** The $omamA_{mtb}$ gene was engineered in frame with an HA tag and expressed in *M. smegmatis*. Cells were lysed to generate whole cell lysates (WCL) and fractionated by differential ultracentrifugation into cell wall (CW), cell membrane (MEM), and cytoplasmic containing soluble (SOL) fractions. Results are representative of at least three independent replicates. **D.** Phyre 2, an online structural prediction program, predicted with high confidence (96%) that OmamA forms a NTF2-like fold. Ribbon diagrams shown represent the Phyre 2 predicted structures of OmamA colored by secondary structure in Pymol. Ribbon diagrams representing the solved crystal structures of VirB8 from *Brucella suis* and DotI from *Legionella pneumophila* are shown for comparison. Alpha helices are colored in red, Beta-strands in yellow, and turns in green.

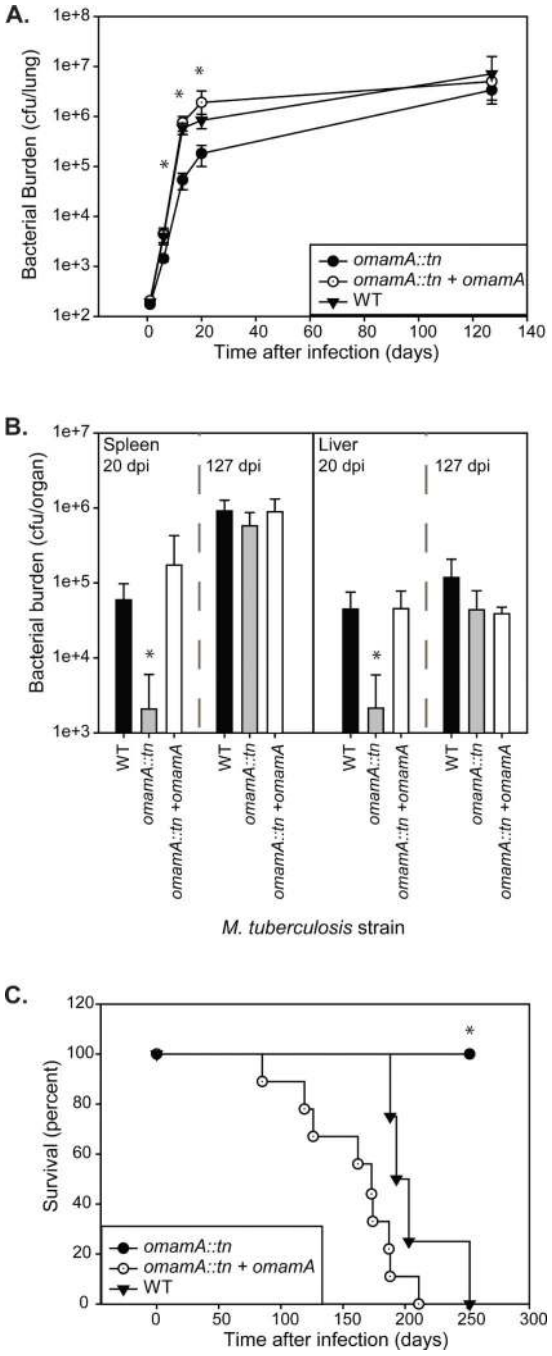

Figure 2.

OmamA is required for early growth and virulence during murine infection. C57BL/6 mice were infected with a low dose aerosol of WT, *omamA::tn*, or *omamA::tn +omamA* complemented strains. Groups of four mice per strain were sacrificed at various days post infection (dpi) and bacterial burden (colony forming units, cfu) was assessed by plating from **A.** lung homogenates or **B.** spleen and liver homogenates. No significant differences were observed in the initial lung burden determined one day post infection (WT 193 +/− 10, *omamA::tn* 174 +/− 9 and *omamA::tn +omamA* 206 +/− 18). **C.** Groups of mice were

monitored for survival. * indicates $p<0.05$ as compared to WT. tn indicates transposon insertion. Error bars represent standard deviation. Results are representative of two independent experiments comparing WT (MBTB178), *omamA::tn* (MBTB319), and *omamA::tn* + *omamA* (MBTB320).

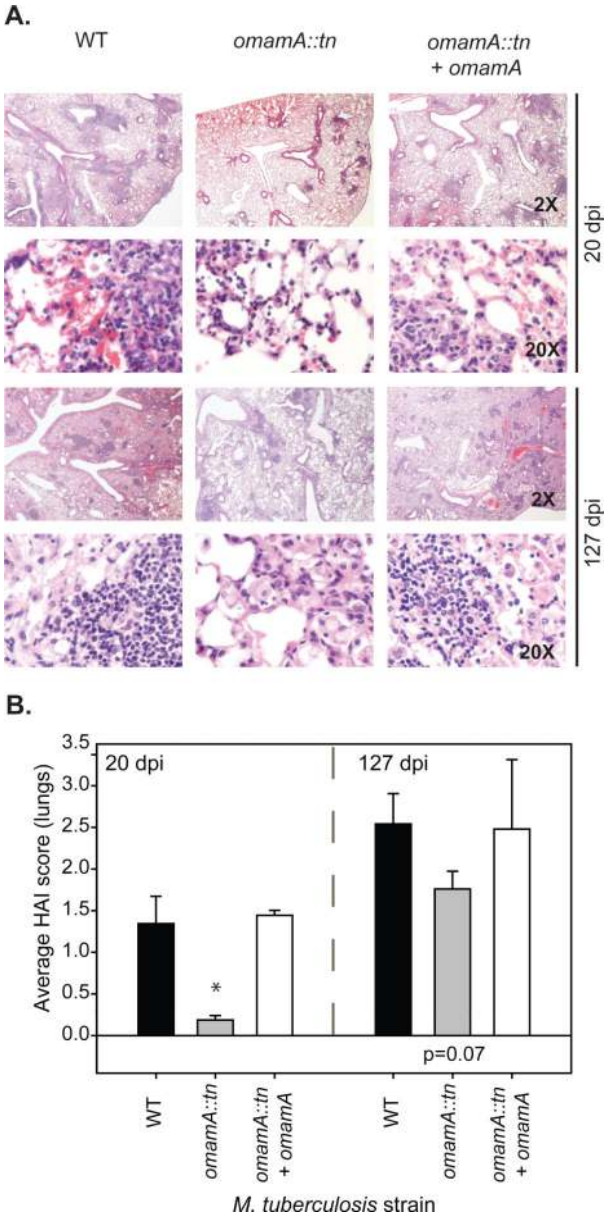

Figure 3.

Mice infected with the *omamA* mutant have reduced histopathology compared to WT infected mice. **A.** A single lung lobe from was fixed and H&E stained for histology. Shown are representative images captured under 2X and 20X magnification from 20 and 127 days post infection comparing WT (MBTB178), *omamA::tn* (MBTB319), and *omamA::tn* + *omamA* (MBTB320). **B.** Average histological activity index (HAI) scores were determined by an experienced blinded reviewer.

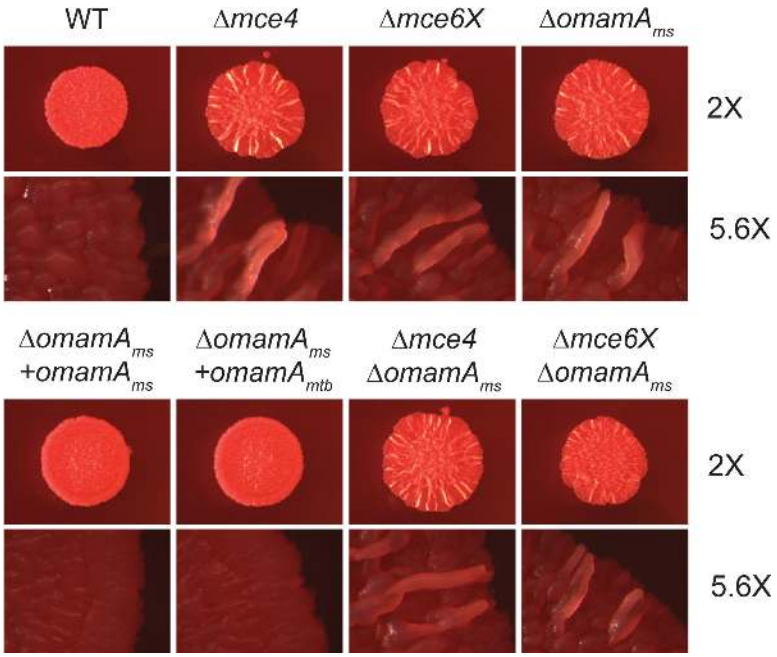

Figure 4.

The *omamA*$_{ms}$ mutant shares a morphology phenotype with *mce* operon mutants. Two μL spots of culture were plated on Mueller Hinton plates containing glucose and Congo red. The resulting colonies were visualized after 2 days at 2X and 5.6X magnification (Leica M420 macroscope). Results are representative of at least three independent experiments comparing WT +pMV261 (EP1182), *Δmce4* +pMV261 (EP1204), *Δmce6X* +pMV261 (EP1208), *ΔomamA* +pMV261 (EP1193), *ΔomamA* +*omamA*$_{ms}$ (EP1194), *ΔomamA* +*omamA*$_{mtb}$ (EP1203), *ΔomamAΔmce4* +pMV261 (EP1206), and *ΔomamAΔmce6X* +pMV261 (EP1210). pMV261 is an empty vector, *omamA* expression constructs are cloned in pMV261.

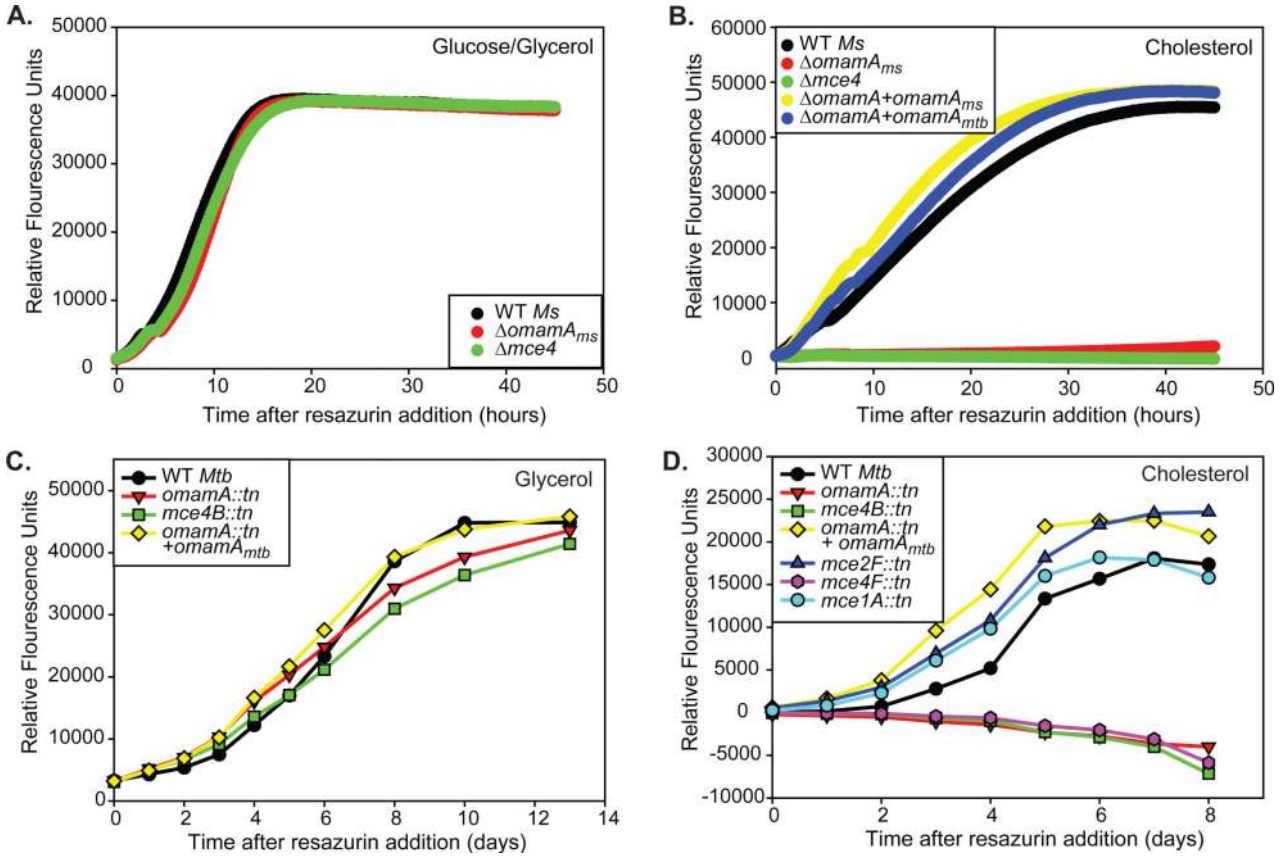

Figure 5.

OmamA is required for *M. smegmatis* and *M. tuberculosis* to utilize cholesterol. **A.** 10^4 colony forming units (cfu) of *M. smegmatis* strains were added to M9 glucose/glycerol and metabolic activity was monitored by resazurin conversion over time. **B.** 10^4 cfu of *M. smegmatis* were added to minimal M9 media plus cholesterol, and metabolic activity was monitored by resazurin conversion over time. Relative fluorescence unit measurements in cholesterol media are reported after subtraction of the minimal signal from no carbon source. 10^4 cfu of *M. tuberculosis* were added to minimal Sauton's media supplemented with **C.** glycerol or **D.** cholesterol, and metabolic activity was monitored by resazurin conversion over time. Relative fluorescence unit measurements in cholesterol media are reported after subtraction of the minimal signal from no carbon source. Results are representative of at least three independent experiments. *M. smegmatis* (*Ms*) strains: WT +pMV261 (EP1182), *Δmce4* +pMV261 (EP1204), *ΔomamA* +pMV261 (EP1193), *ΔomamA +omamA*$_{ms}$ (EP1194), and *ΔomamA +omamA*$_{mtb}$ (EP1203). *M. tuberculosis* (*Mtb*) strains: WT (MBTB178), *omamA::tn* (MBTB319), *omamA::tn + omamA* (MBTB320), *mce2F::tn* (MBTB156), *mce1A::tn* (MBTB204), *mce4B::tn* (MBTB329), *mce4F::tn* (MBTB288).

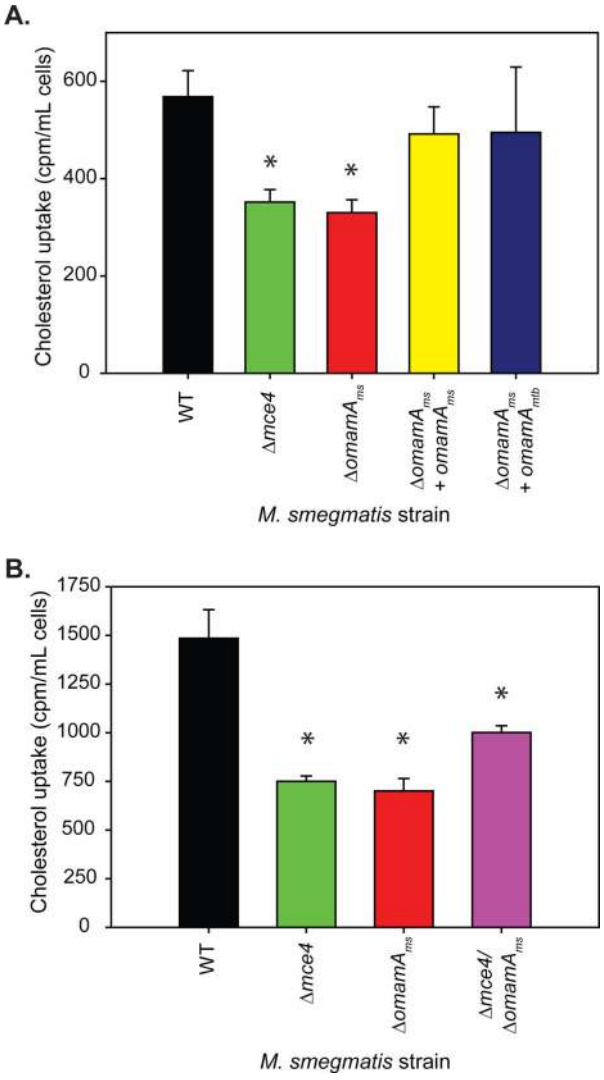

Figure 6.

OmamA is required for cholesterol uptake. **A.** and **B.** *M. smegmatis* strains were grown overnight in M9 glucose/glycerol, and washed extensively in M9 no carbon source. Cells were incubated with 4-C^{14}-cholesterol for two hours, washed extensively, and cell associated radioactivity levels were measured by scintillation counter. * indicates $p<0.05$ compared to WT. Error bars represent standard deviation. Results are representative of at least three independent experiments. *M. smegmatis* strains: WT +pMV261 (EP1182), *Δmce4* +pMV261 (EP1204), *ΔomamA* +pMV261 (EP1193), *ΔomamA* +$omamA_{ms}$ (EP1194), *ΔomamA* +$omamA_{mtb}$ (EP1203), and *ΔomamAΔmce4*+pMV261 (EP1206).

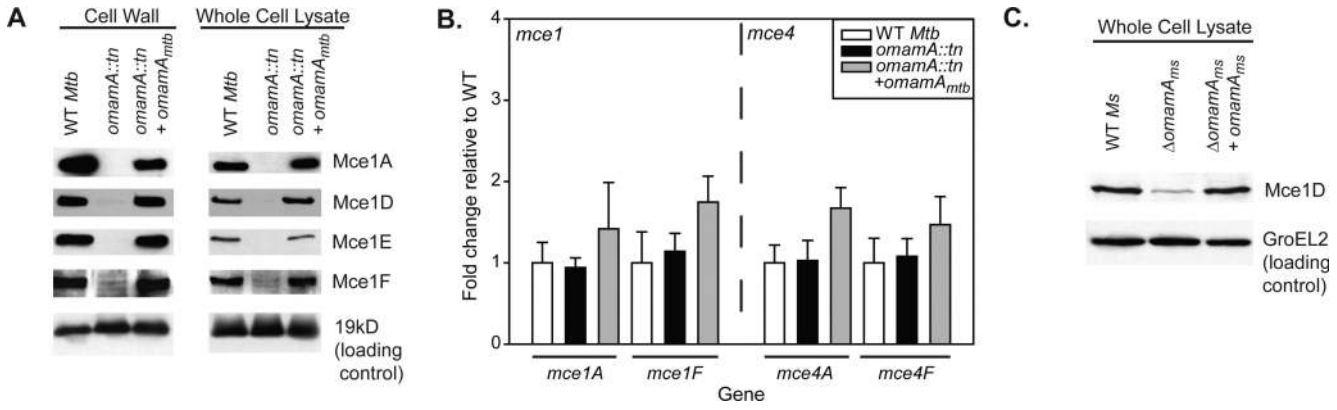

Figure 7.

Mce1 protein levels are reduced in the absence of OmamA. **A.** *M. tuberculosis* (*Mtb*)cells were irradiated and lysed by French press to generate whole cell lysates (WCL) and fractionated by differential ultracentrifugation into cell wall fractions. Western blots were performed for Mce1A, Mce1D, Mce1E, Mce1F, and the 19kD lipoprotein with equal protein amount loaded across strains. Results are representative of at least three independent replicates. **B.** RNA was collected from *M. tuberculosis* WT, *omamA::tn*, and *omamA::tn* +*omamA* complemented strains and transcript levels of *mce1A*, *mce1F*, *mce4A*, and *mce4F* were determined by Quantitative Real-Time PCR and normalized to expression of the housekeeping protein *sigA* (Manganelli *et al.*, 1999). Reported are fold change values for each gene relative to expression in WT *M. tuberculosis*. Error bars represent standard deviation. Results are representative of at least three independent experiments with WT (MBTB178), *omamA::tn* (MBTB319), and *omamA::tn* + *omamA* (MBTB320). **C.** *M. smegmatis* (*Ms*) cells were lysed by glass beads to generate whole cell lysates (WCL). Western blots were performed for Mce1D and GroEL2 with equal protein amount loaded across strains. Results are representative of at least three independent experiments with *M. smegmatis* WT +pMV261 (EP1182), *ΔomamA* +pMV261(EP1193) and *ΔomamA* +$omamA_{ms}$ (EP1194) strains.

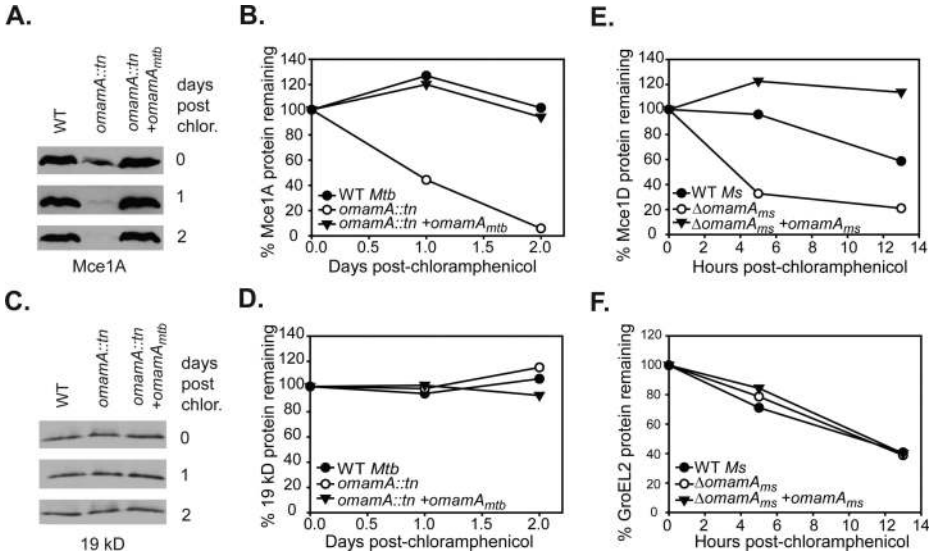

Figure 8.

Mce1 proteins are stabilized by the presence of OmamA. Cultures of *M. tuberculosis* (*Mtb*) and *M. smegmatis* (*Ms*) were treated with chloramphenicol to prevent further protein synthesis and protein stability was monitored over time by Western blot analysis of whole cell lysates (WCL) with equal protein amount loaded across strains and timepoints. Samples were removed at specific time points, formalin fixed (for *M. tuberculosis*) and lysed by glass beads to generate WCL. **A.** The stability of Mce1A in *M. tuberculosis* strains was followed over a two day time course by Western blot analysis. **B.** Mce1A protein decay was quantified by measuring band intensity on Western blots using ImageJ. **C.** The stability of the exported 19 kD lipoprotein in *M. tuberculosis* over time as monitored by Western blot. **D.** 19 kD protein abundance was quantitated by ImageJ. Results are representative of at least two independent experiments with *M. tuberculosis* WT (MBTB178), *omamA::tn* (MBTB319), and *omamA::tn* + *omamA* (MBTB320) strains. **E.** Decay of Mce1D was quantified in *M. smegmatis* cultures over 13 hours by measuring band intensity on Western blots using ImageJ. **F.** Decay of GroEL2 was quantified in *M. smegmatis* cultures over 13 hours by measuring band intensity on Western blots using ImageJ. Results are representative of at least three independent experiments with *M. smegmatis* WT +pMV261 (EP1182), *ΔomamA* +pMV261 (EP1193) and *ΔomamA* +$omamA_{ms}$ (EP1194) strains.

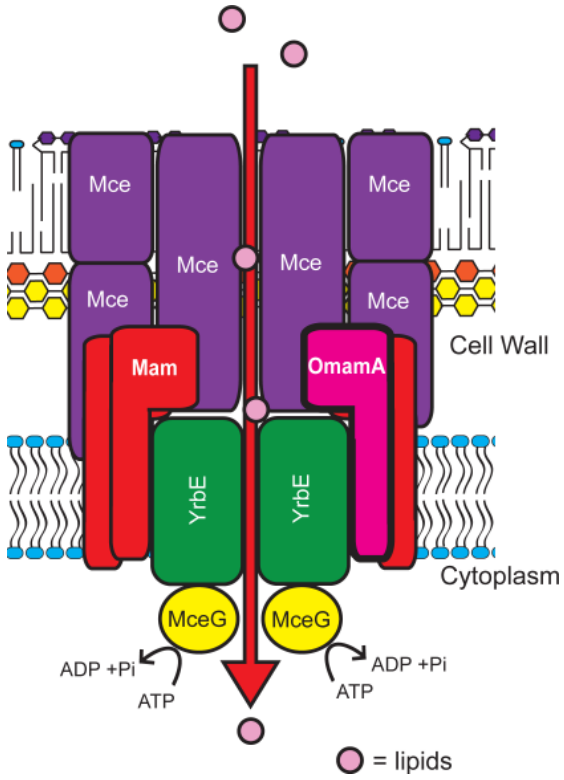

Figure 9.

OmamA is an integral membrane protein that is important to Mce transporter stability and function. OmamA (pink) and other Mam proteins (red) are embedded in the inner membrane by an N-terminal transmembrane domain with the majority of the protein being localized on the cell wall side of the membrane. Mce permease proteins (YrbE), shown in green, are multi-membrane spanning proteins localized to the inner membrane. Some Mce proteins contain predicted TM domains; however, localization from this and other studies (Klepp *et al.*, 2012) suggests that Mce proteins are located within the cell wall (shown in purple). MceG, shown in yellow, is the cytoplasmic Mkl family ATPase predicted to be responsible for ATP-hydrolysis that powers the transport of substrates, shown in light pink, through the complex.